Table of Contents

Table of Figures

Table of Tables

Acknowledgments

I would like to thank my advisor, Dr. Qi Wen, for setting me on my path and providing me with all the guidance necessary to succeed in this endeavor.

I would like to thank my thesis committee members, Dr. Kristen Billiar and Dr. Raymond Page, for taking the time to collaborate with me and helping me refine the focus of my research.

This project has been ongoing for a long time, and as such, a lot of people have had a chance to contribute in large and small ways. For their contributions to the protocol I would eventually formulate and use for my research, I would like to thank Mina Shojaeizadeh, Xuyu Qian, and Prashant Yamajala. For teaching me everything I needed to know about immunohistochemical staining, I would like to thank Jason Forte. For his overall helpfulness all throughout my tenure in Dr. Wen's lab, I would like to thank my fellow lab mate Gawain Thomas.

Lastly, I wish to thank my family for supporting me throughout my education, as well as for being understanding and comforting when things did not always go as planned.

Abstract

Cell traction force is generated in the cytoskeleton by actomyosin activity and plays an important role in many cellular processes. In previous cell traction force experiments performed by our lab, unexpectedly large variations were measured. Because these experiments were utilizing a cell population of randomized phase, and there had been no documented investigation into whether cell phase affected cell traction force generation or propagation, it was hypothesized that there would be a significant difference in traction force between S phase and the other phases of interphase, as the physical and chemical changes happening within the nucleus at this time might elicit changes within the cytoskeleton. To test this hypothesis, we characterized the time-evolution of traction forces from a population of synchronized 3T3 fibroblasts. 3T3 fibroblasts were synchronized in G1-phase via serum starvation. The transition times between cellular phases during the first cell cycle after synchronization were identified by BrdU and Hoechst staining at different time points. After phase transition times were approximated, the traction forces of 9 cells were measured in 4-hour intervals for 24 hours. The differences between traction forces measured in G1, S, and G2 phases are not significant, demonstrating that cellular phase does not significantly affect traction force magnitude.

1.   Introduction

1.1.   The Cell Cycle

The cell cycle is a process in which a healthy cell grows, synthesizes DNA, then divides into two separate cells, each approximately the same size. Most cells will, after many cell cycles, begin to show signs of aging and cease dividing. This end to proliferation is called senescence.[11] However, certain types of cells, such as rat 3T3 fibroblasts, are mutated to the degree that they are considered "immortal," meaning that, under the right circumstances, they have the potential to divide continuously.[11]

The cell cycle is split between two major components, interphase and M-phase. Interphase lasts much longer and is made up of three distinct sub-phases, which are G1, S, and G2 phase. At G1 phase, the cell may grow in size but maintains a constant quantity of DNA in its nucleus. The amount of chromatin in this phase is referred to as "2N," as each strand of DNA has a complimentary strand, forming a double helix. Also of note, centrioles, structures that play an important role in cell division, are replicated in this phase.[1] During S phase, the cell produces new strands of DNA. DNA strands unravel from structures in the nucleus called histones and unbind from each other.[1] A new complementary strand is synthesized for each preexisting strand, forming new double helices.[1] When G2 phase is reached, the cell's chromatin has reached a state of "4N," as it has doubled. DNA condenses back into the form of double helices, but there are twice as many in G2 phase as in G1.[1]
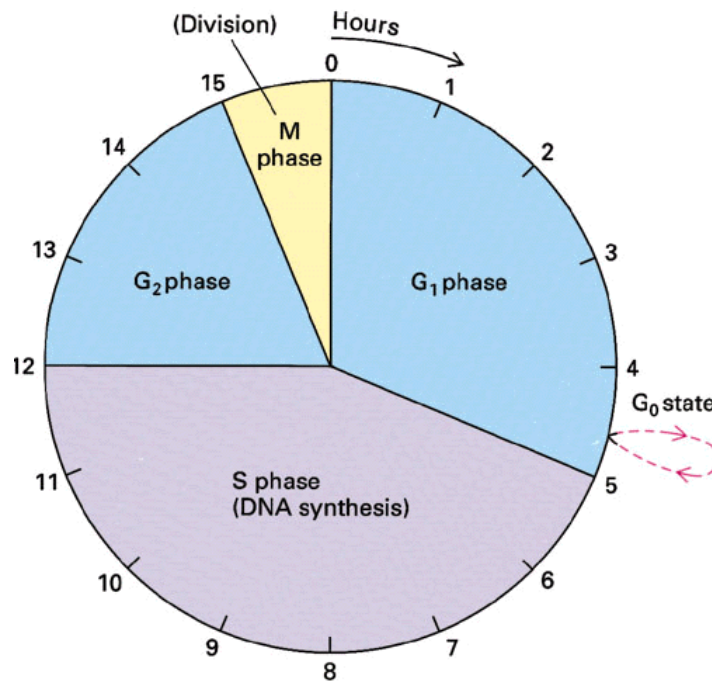
Figure 1: Diagram of a 16-hour cell cycle, roughly the doubling time of NIH-3T3 fibroblasts [15].

After spending time in G2 phase, the cell will begin M-phase, better known as mitosis. M-phase, like interphase, has several sub-phases, but these occur more rapidly. It begins with prophase, which involves the chromatin condensing into chromatids.[1] In metaphase, the nuclear envelope dissolves and the chromatids are aligned along the center of the cell.[1] During anaphase, the chromatid pairs are pulled apart, half of each chromatid being pulled towards their respective centrosome.[1] Finally, telophase is reached, at which point the cell begins to divide. A cleavage furrow forms at the center of the cell, leading eventually to cytokinesis, the point at which the cell split into two separate cells.

Oftentimes, after finishing mitosis, a cell will enter G0 phase instead of G1 phase. G0 phase is not considered part of the cell cycle.[15] During G0 phase, the cell is not undergoing any sort of activity relative to dividing. It will remain in G0 phase until it is given a signal to divide, at which point it may reenter G1 phase and continue the cell cycle.[15]

1.2.   Synchronization of Cell Cultures

In order to identify cell phase in a population, staining techniques must be employed. However, staining a population of cells that is unsynchronized will not yield any poignant data. The simplest way to synchronize a population of cells within the same phase is by reducing the concentration of growth factors and serum within their medium and allowing them time in these conditions in order to pass through one cycle and come to rest.[11] At this point, the cells will all be within either G0 or G1 phase. With the reintroduction of normal serum levels, most cells will slowly return to the cell cycle, but those that return to it will all be within the same phase at the same time. The degree of synchronization will decrease with each cell cycle due to slight variations between each cell's respective cycles.

1.3.   The Cytoskeleton

The cell's cytoplasm is given shape and motility by its cytoskeleton. The cytoskeleton is made up of microfilaments, intermediate filaments, and microtubules.[4] The cytoskeleton's terminal point is at the cell membrane, where it is most often bound to surface receptor proteins, like integrins. When an integrin binds to a ligand outside the cell, it can be referred to as a focal adhesion. Forces and signals can pass into and out of the cell through focal adhesions.[4]

1.4.   Integrins

Cell surface proteins known as integrins are responsible for the detection of and reaction to environmental characteristics and changes. Every cell type has an abundance of integrins, of varying types and quantities. The main job of an integrin is to bind to a ligand, which will most often be part of the extracellular matrix.[2] Doing so will typically elicit some sort of response

from the cell and create a focal adhesion, which the cell can use to act on its surroundings. Each type of integrin has an affinity for certain ligands.[2] If a cell has more of one type of integrin than another, it may bind more readily to one type of ligand than to another due to integrin affinities. Additionally, many integrins have an affinity for multiple types of ligands, meaning that they are able to bind to a variety of molecules rather than a single type, thought they can only bind to one at a time. For instance, the integrin α2β1 can bind to collagen, fibronectin, and laminin.[3] Meanwhile, integrin α1β1 will bind to collagen and laminin, but will not do the same for fibronectin.[3]

With regards to traction force, integrins can play a huge role in determining both the magnitude and direction of stresses applied by a cell. They serve as the point at which a mechanical signal can enter the cell, as well as the point at which the mechanical response will exit the cell. Furthermore, integrin affinity can greatly influence a cell's ability to exert traction force, as focal adhesions are required for a cell to do so.

1.5.   Mechanotransduction

Cells are capable of sensing both chemical and physical signals, as well as responding with chemical and physical reactions. An example of a chemical signal would be the presence of a growth factor, and the cell's response may be to differentiate.[5] Physical signals can have effects on cells much the same as chemical signals can. The process by which cells sense and react to mechanical stimuli is called mechanotransduction. The first step in mechanotransduction is mechanosensing.

Mechanosensing begins at the focal adhesion, a bond between a cellular surface protein called an integrin and a ligand. The signal travels into the cell through the integrin and propagates along any attached cytoskeletal filaments.[4] The terminal point of many cytoskeletal filaments is the nuclear envelope, so many integrins are linked to the nuclear membrane through the cytoskeleton.
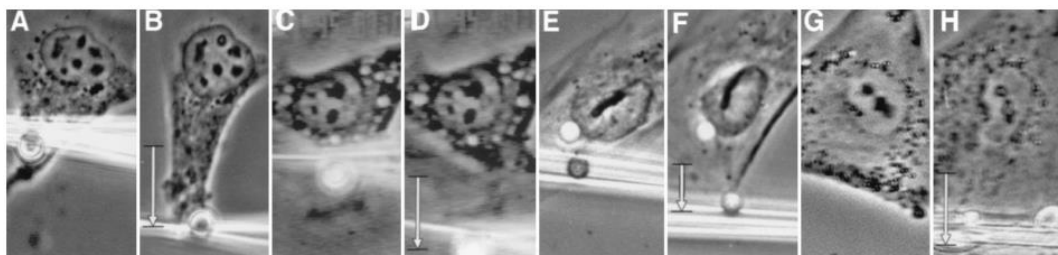
Figure 2: A demonstration of nuclear movement and deformation caused by deformation of the cell membrane via pulling [4].

In terms of physical signals, the two most commonly sensed and reacted to by cells are external forces and matrix stiffness. In reaction, a cell may alter its cytoplasmic stiffness, exert its own forces, or even migrate from its initial position.[5]
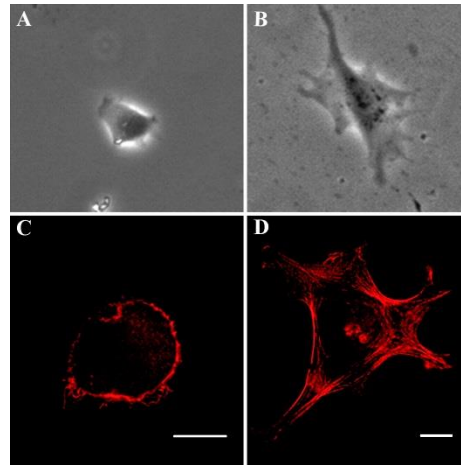
Figure 3: An example of how a soft gel (images A and C) and a stiffer gel (images B and D) effect stress fiber development, cell shape, and cell size [8].

1.6. Traction Force

Eukaryotic cell motility is achieved through traction force. Cellular traction forces are the forces generated by a cell and applied to an adjacent surface or the surrounding environment, which are used to pull the cell forward. When applying a traction force, a cell must contract part of its cytoskeleton via myosin motors. Myosin motors, when activated by the hydrolysis of Adenosine triphosphate (ATP), bind to nearby strands of actin and pull on them.[1] A series of myosin motors and cytoskeletal microfilaments allow the cell to manipulate its own cytoplasm and cell membrane in order to act on its environment.

Besides myosin motors and cytoskeletal filaments, a cell must also have the proper integrins to generate traction force. Integrins are proteins in the cell membrane which are typically connected to microfilaments in the cytoplasm. On the side facing out of the cell, they are able to come into contact with and bind to various ligands of the extracellular matrix. The extracellular matrix is a dense network of large molecules both created and inhabited by cells. The extracellular matrix has a wide variety of uses for the cell, including a transit network and a means of cell-to-cell signaling. When an integrin binds to a component of the extracellular matrix, it is able to communicate certain information to the cell and also now serves as a point from which the cell may exert force on its surroundings. This binding site is called a focal adhesion. The cell, by activating many myosin motors in tandem and causing the contraction of filaments, can pull on this focal adhesion in order to move itself in a specific direction.[6] When enough focal adhesions are engaged, this action is what allows the cell to migrate.
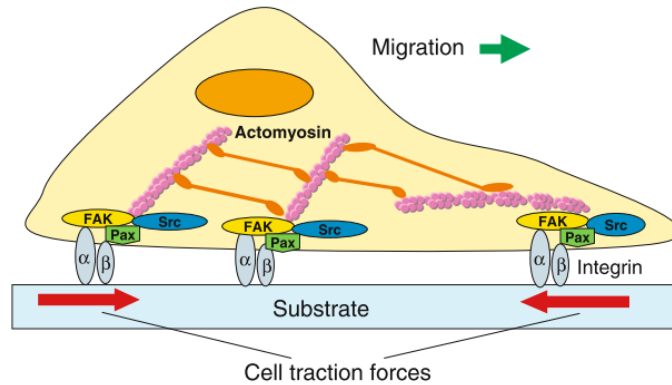
Figure 4: Diagram of a cell migrating along a substrate [6].

In order for the cell to migrate, it constantly creates new focal adhesions and relinquishes old ones. The leading edge of the cell is the edge which is advancing forward, while the trailing edge is opposite the leading edge. The leading edge is where most new focal adhesions will form, whereas the trailing edge is where focal adhesions will be disconnecting in order for the cell to move forward. Because the cell is in an equilibrium of forces at any instant, large stresses are applied to the substrate through both the leading and trailing edges of the cell.

1.7.   Cell Traction Force Trends

Cell traction force can differ greatly from cell to cell. Certain relationships between traction force and other variables have been discovered and documented. One such variable which shares a relationship with traction force is spreading area. In two-dimensional culture, a cell's spreading area is simply its top-down visible area on a substrate. Generally, a cell's spreading correlates to its traction force; cells which spread out further typically produce greater forces.[7,10] As larger cells can spread wider, it can also be said that generally larger cells are capable of producing more force than smaller cells.

Besides size, a cell's shape also plays a part in its motility and force generation. Typically cellular shape is expressed numerically by a value known as circularity. Circularity is a measure of how closely a shape resembles a circle, and is defined by the following equation:

$$Circularity = \frac{4\pi * Area}{Perimeter^2}$$

Circularity is a unitless value ranging between 0 and 1. A perfect circle would have a circularity of 1. Typically, cells on a substrate produce more force when they have lower circularities, although how low they can get depends on the kind of cell. A low circularity oftentimes indicates an elongated phenotype or many branching filopodia.[9] A high circularity may indicate that the cell is dying, cannot bind to its substrate, or is about to enter mitosis.

13

Another way in which cell shape can be quantified is through the cell's elongation index, which is defined by the equation:

$$Elongation\ Index = \frac{Major\ Axis}{Minor\ Axis}$$

Typically the major axis is defined as the length between the leading and trailing edges of the cell, whereas the minor axis is the width of the cell at its center, usually marked by the presence of the nucleus. Elongation index has a minimum value of 1, which would indicate that the major and minor axes are equal in length. If a cell was measured to have an elongation index close to 1, it would most likely have a circular phenotype. Since more circular phenotypes typically produce lesser traction force, a higher elongation index usually produces greater force than one with a lower elongation index.

It has been noted that cells on stiffer substrates produce more forces, spread wider, and have less circular morphologies than those existing on soft substrates.[7,8,10] It has even been documented that some cells tend to migrate from areas of low stiffness to areas of high stiffness, but will not migrate from areas of high stiffness to areas of low stiffness.[8]

The presence of other cells can have an effect on cellular traction force as well. Cells have a variety of ways to interact and communicate, but when they come in contact with one another, it has been observed that they may actually act in unison and produce forces greater than the sum of what they were producing prior to coming into contact.[10]

1.8. Fibroblasts

Fibroblasts are a type of cell which produces the precursors of several important structural proteins in order to form new extracellular matrix.[12] This ability makes them extremely important in the developmental stages of life and in the process of wound healing. They are most often found in connective tissues.[12]

Fibroblasts start out as fibrocytes, an inactive form with low mass and mobility.[12] After maturation, fibroblasts will migrate based on extracellular chemical signaling. For instance, necrotic cells can release molecules that direct fibroblast migration, leading the fibroblasts to damaged tissue in need of repair. Some examples of these signaling molecules are HMGB1 and (SDF)-1/CXCL12.[13] Apoptotic cells, on the other hand, do not release these molecules, thus fibroblasts will not respond to their deaths. Similar signals guide fibroblasts during the development of new tissues in organisms during development.

Fibroblasts play a role in chronic inflammation. Chronic inflammation can result in widespread tissue damage and lasts for extended periods of time, requiring fibroblast participation to keep tissues semi-functional as the immune system works to remove the perceived threat which caused the inflammatory response. If the inflammatory response requires

the creation of an abscess to remove the threat, fibroblasts additionally are partly responsible for forming its walls.[14]

The reason fibroblast traction force is so important is because of the nature of their work. Fibroblasts must migrate through tissues constantly in order to perform their duties during development and wound healing.

1.9.   Traction Force Measurement

Cell traction force was first proven to exist in 1980, when a group showed that cells were able to wrinkle a silicone membrane.[16] Since then, many scientists have devised various ways of quantifying cellular traction force in order to discover new trends and interplay between cellular traction force and other variables. The majority of these methods involve measuring the displacements caused by cells at points along the surface on which they reside.

One means of measuring cell traction force is to create a micro-patterned gel with an array of microscopic pillars and culture cells on them. The cells pull on the pillars, particularly on those that are on the outer border of the cell. As the length and modulus of elasticity of the pillars are both known, only the deflection and moment of inertia must be determined in order to solve for the force applied on each pillar.[17]

The second method, which will be the focus of this paper, involves a flat gel of known stiffness with fluorescent microbeads embedded in its surface. The gel is coated with a specific type of ligand or a mix of ligands and then cells are cultured on top of it. Images of the locations of beads can be taken when the cells are off and on the gel. From these differing images, a displacement field can be produced. As the strain and elastic modulus of the gel are both known, a stress field can then be created and analyzed.[10]

More recently, methods have been designed to monitor cell traction force in a 3D environment. Whereas in the previous methods described, the cells were cultured on a surface, these cells are cultured within a hydrogel. The hydrogel is interspersed with fluorescent markers, so a scanning confocal microscope is used to image 3D models of the gel and again displacements of the markers can be analyzed in order to quantify stress and force data.[18]

1.10. Motivation from Previously Collected Data
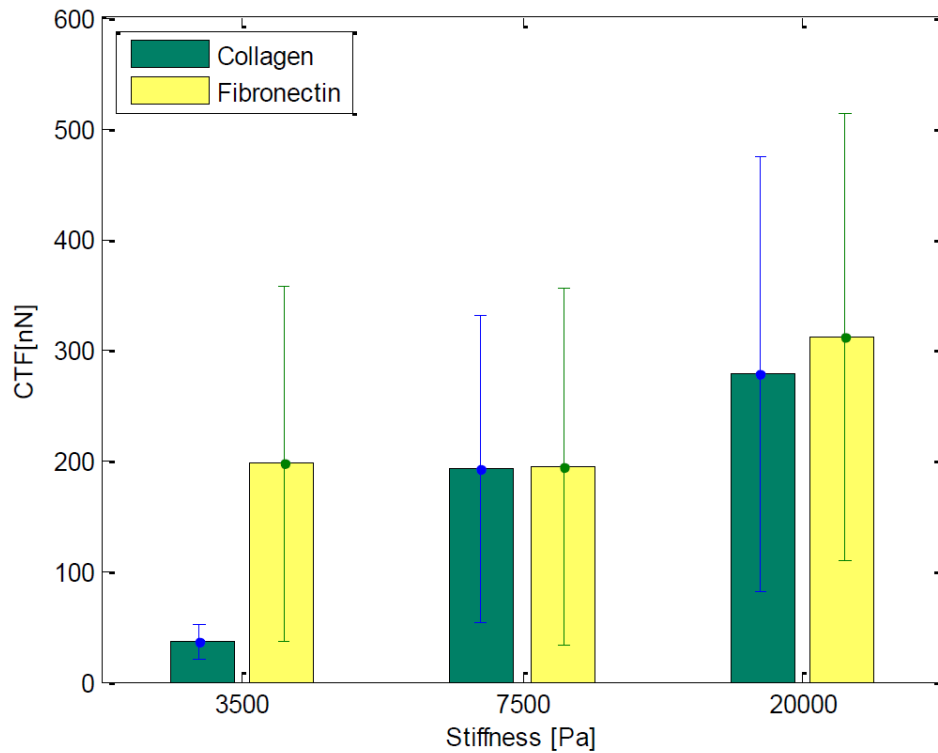
Figure 5: Cell traction force results for 3T3 fibroblasts seeded on gels with varying stiffnesses and coatings [28].

Previously collected data in our lab had very high degrees of variance, which proved problematic. For instance, were it not for the degree of variation displayed in Figure 5, the averages might lead us to the conclusion that fibroblasts seeded on a 20 kPa stiffness gel will exert more force than those seeded on a 7.5 kPa gel.

Trying to make sense of the variation led us to a few ideas for future experiments. First, there could be a factor at play we are unaware of that needs to be the focus of its own experiment. Secondly, if cell traction force is known to fluctuate with time, taking single time point measurements of a group of cells is inviting randomness. Ideally selected cells would be tracked and have their traction forces measured at multiple time points in order to ensure that we were not measuring some cells at their weakest point while simultaneously measuring others at their strongest. Lastly, it was possible that some cells would simply generate more or less traction force than their peers throughout their existence, so again it would be better to have multiple time points so that we could better characterize each cell and possibly normalize the data in order to mitigate this factor.

1.11. Hypothesis and Aim

Our findings suggested to us that an unknown factor was influencing our data and causing problematic variance. Cell phase was randomized in our experiments, and there was very little information available about how cell traction force might change throughout the cell cycle. It was hypothesized that cell traction force would be generated at a lower magnitude during S phase than G1 or G2 phase. The idea that the forces exerted would lessen during this phase came from the notion that the nucleus may become less stiff or grow slightly in volume to house extended DNA molecules during DNA synthesis. A change in nuclear stiffness could have a slight impact on the overall tension of the cell's cytoskeleton, as some components of the cytoskeleton are linked to the nucleus. If the nucleus expanded in size, it could push some cytoskeletal components out of their initial configuration, which might lead to the cell being unable to exert force on its surroundings in the same way it was able to previously.

We decided to investigate the influence of cell phase on traction force ourselves by synchronizing a cell population and taking multiple cell traction force readings of specific cells over the course of a cell cycle. To supplement this data, we would use cell staining to determine the phase transition timings of the cells so that traction force data could be properly attributed to its corresponding phase.

2. Methods

2.1. Cell Culture

Rat NIH 3T3 fibroblasts were maintained at 37° C and 5% CO_2 in Dulbecco's Modified Eagle's Medium (Lonza-BioWhittaker®) supplemented with 10% Fetal Bovine Serum, 1% penicillin-streptomycin, and 2 mM L-Glutamine.

When cells in culture reached 90-100% confluency, their medium was aspirated. The dish was rinsed with warm PBS (Lonza-BioWhittaker®) and left to rest for two minutes. The PBS was then aspirated and replaced with 5 mL PBS containing 0.01% trypsin (Gibco®). The dish was left to rest inside the incubator for a few minutes. The contents of the dish were pipetted up and down a few times to properly raise the detached cells into suspension, then the contents were pipetted into a centrifuge tube with an additional 5 mL of cell culture medium. The tube was centrifuged for 6 minutes at 1600 RPM. After this point, excess fluid was aspirated, the cell pellet was re-suspended in culture medium, and the cell concentration was approximated with a hemocytometer.

For cell staining, the cells were seeded in four-well plates with collagen-coated wells. A 200 μg/mL collagen solution was produced from PBS and an initial 9.47 mg/mL solution of rat tail collagen (BD Biosciences). 0.5 mL of the solution was pipetted into each well and left to rest for 1 hour. The wells were lightly rinsed with PBS and aspirated before cells were seeded in them. Based on the area of each well and the desired cellular concentration for experiments, approximately 2350 cells were seeded in each well.

For cell traction force experiments, the cells were seeded into a customized petri dish with a hydrogel glued into its center. The dish was 55 mm in diameter and it was decided that about 31,500 cells would be the ideal number to seed in each dish used for this purpose.

Cells not needed for experiments were used to continue the cell line in a new petri dish, starting at about 10% confluency. Excess cell suspension was discarded through aspiration.

2.2. Cell Starvation

After the experimental cells had a few hours to adhere to a surface, their medium was aspirated and replaced with 2% FBS medium, then returned to the incubator. After two more hours, the medium was again replaced, this time with 0.5% FBS medium, and the cells were returned to the incubator. After two more hours, the medium was aspirated and the dishes or well plates were rinsed with warmed PBS. After two minutes, the PBS was aspirated and replaced with 0.2% FBS medium. The PBS rinse was to ensure that very little residual medium remained in the dish when the 0.2% FBS medium was added, as it was important that the serum concentration was not any higher than 0.2%. The cells were put back in the incubator and left

there for 48 hours. The final serum concentration and incubation time were based on a protocol were based on C. Schorl and J. Sedivy.[19]

After the starvation period, cells were reintroduced to 10% serum medium. In the case of cells meant for staining, bromodeoxyuridine (BrdU) labelling reagent was added to their medium in a 1:100 dilution. During DNA synthesis, BrdU replaces the nucleoside thymidine.[20] This means that it will chiefly be expressed in cells that are in or have passed through S phase since the introduction of the BrdU labelling reagent. To find when a synchronized population of cells will reach S phase, BrdU labelling reagent can be introduced to multiple cultures after synchronization and each culture could be fixed at different time points, then stained to detect which had reach S phase (positive expression of BrdU) and which had not (negative expression of BrdU).

2.3.   Cell Fixation

Cells used in staining experiments were fixed periodically. Every well in a well plate was fixed simultaneously. First, medium was aspirated and replaced by 1 mL of Ca^{2+}/Mg^{2+} augmented PBS per well. After 10 minutes, the PBS was aspirated and 0.5 mL cold methanol was introduced to each well in order to fix the cells. After 15 minutes, the wells were washed three times with 0.5 mL PBS each, allowing the PBS to rest in the wells for 5 minutes at a time. The PBS was aspirated and replaced with 0.5 mL of 0.1% sodium azide in PBS for each well. The well plates were then sealed with Parafilm® and refrigerated at 4° C.

2.4.   Cell Staining

PBS was aspirated from all the wells. 0.5 mL of 1.5N HCl were added to each well. After 10 minutes, the HCl was aspirated and the wells were washed three times with 1.0 mL .05% Tween-20 in PBS, allowing the PBS-Tween to rest in the gels for 5 minutes at a time, in order to neutralize the HCl.

Next, the samples were blocked in 5% goat serum in PBS-Tween for 15 minutes. The purpose of blocking is to occupy potential binding sites of the primary or secondary antibodies required for staining in order to prevent non-specific binding, which will allow for clearer images. After blocking, the wells were aspirated and then incubated with the primary BrdU antibody, G3G4, in PBS-Tween for 30 minutes.

The samples were aspirated, washed with PBS-Tween three times allowing 5 minutes for the PBS to rest in between each rinse, and then were incubated for half an hour, this time with a 1:500 dilution of the fluorescent secondary antibody, goat anti-mouse IgG, in PBS-Tween. The fluorescence of this antibody can lose its intensity if exposed to light, so all unnecessary lighting was turned off and the samples were covered in aluminum foil during this time.

The cells were next aspirated and washed four times with 0.5 mL of PBS in each well. The cells were then counterstained with Hoechst stain at a concentration of 0.5 µg/mL, 0.5 mL per well, for 10 minutes. Finally, the wells were aspirated, washed with 1 mL of PBS, given 0.5 mL of 0.1% sodium azide in PBS, and wrapped in aluminum foil for later observation.

2.5.   Analysis of Stained Cells

Cells stained with BrdU and Hoechst were imaged on a microscope. BrdU-positive cells were stained green, and thus were visible under the FITC fluorescent spectrum, whereas Hoechst-positive cells were stained blue, and thus were visible under the DAPI setting.

Six images were taken for each batch of cells fixed at a specific time point. Cells that were BrdU-negative were considered to be in G1 phase, while BrdU-positive cells were considered to be in S or G2 phase. Hoechst was used as the guideline for keeping track of population proliferation, as all cells would be stained positive, and thus the approximate time of mitosis could be gathered from this data.
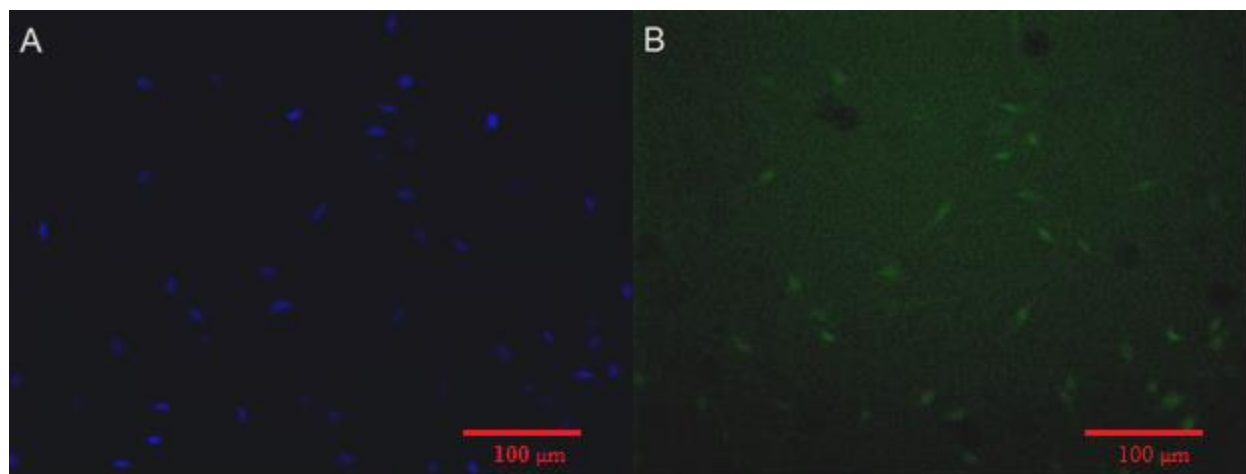
Figure 6: Side-by-side comparison between Hoechst-stained cells (A) and BrdU-stained cells (B). The BrdU stain was fainter than the Hoechst and was more prone to non-specific binding.

2.6.   Making a PDMS Stamp

A PDMS stamp was produced in order to transfer a grid pattern onto the bottom of each gel used in cell traction force experiments. 10 grams of silicone base (Dow Corning Corporation) was measured out and then 1 gram of silicone curing agent (Dow Corning Corporation) was added. The two were mixed thoroughly until any large bubbles had been eliminated, then the mixture was put into a vacuum chamber for 15 minutes in order to eliminate smaller bubbles. Meanwhile, a glass slide etched with a grid pattern was sonicated in ethanol for 5 minutes. After it was dried, it was glued to the interior of a petri dish with the etched grid facing upwards. The

glue utilized was cured with UV light for about 5 minutes. PDMS was poured into the petri dish when it was ready. The petri dish containing the PDMS was placed in a 72° C incubator and left for 2 hours. After this time, the PDMS had solidified. A square was cut into the layer of PDMS around where the grid-patterned glass slide was, resulting in a rectangular piece of PDMS with an etched grid on one side.

2.7.   Preparing Glutaraldehyde-Treated Glass Slides

25x25 mm glass slides were soaked in ethanol and cleaned with a sonicator for five minutes. Next they were placed in a 10% (3-Aminopropyl)trimethoxysilane (Sigma-Aldrich Co.) aqueous solution with a stir bar and stirred for 30 minutes. After this time, the slides were flushed with distilled water and heated in an oven until all water had evaporated. The slides were allowed to cool, and then were placed in a 0.5% glutaraldehyde (Amresco®) bath and refrigerated for a minimum of six hours.

When ready for use, the glass slides were dried. A PDMS stamp was sonicated in ethanol for five minutes and plasma treated for 45 seconds. It was then given two coats of ink on the side with the grid pattern, allowed twenty seconds to partially dry, and then pressed onto a dried glutaraldehyde-treated glass slide continuously for about two minutes before the two were peeled apart. This process was repeated for each gel produced.

2.8.   Preparing Microbead-Coated Glass Slides

A solution of 2% 0.2-micrometer diameter red fluorescent carboxylate-modified microbeads (Invitrogen™) was diluted 1:200 in 1 mL of ethanol. Prior to each use, the tube of bead solution was sonicated for 5 minutes. 25x25 mm glass slides were soaked in a beaker of ethanol and cleaned with a sonicator for five minutes. Next they were dried and plasma treated for 45 seconds. The slides were each coated with 50 microliters of 0.5% bead solution and immediately placed in an oven at 150° C in order to rapidly evaporate the ethanol and leave the microbeads in a relatively uniform layer on top of the glass.

2.9.   Polyacrylamide Gel Synthesis

Polyacrylamide solutions were made up of HEPES buffer (50 mM, pH=8.2), polyacrylamide (Biorad Laboratories), and bis-acrylamide (Biorad Laboratories). The PA solutions prepared were 8% polyacrylamide and 0.1% bis-acrylamide. In order to make gels, 0.9 microliters of tetramethylethylenediamine (Amresco®) and 2.5 microliters of ammonium persulfate (Amresco®) were added to 250 microliters of PA solution. 64 microliters of the gel solution were dropped on glutaraldehyde-treated glass, with the ink grid facing down. A glass slide coated with beads was promptly placed on top of this, with the bead-coated side facing

down in order for beads to be transferred onto the forming gel's surface. After seven minutes, the slides were pried apart, resulting in a solidified gel adhering to the glutaraldehyde-treated slide.

Gels were glued into petri dishes and kept hydrated for extended periods of time with HEPES buffer.

2.10. Polyacrylamide Gel Stiffness Characterization

The polyacrylamide gels used in this experiment were assumed to be isotropic, meaning its mechanical properties were the same throughout and in all directions. Polyacrylamide gels can have a variety of different stiffnesses depending on their acrylamide and bis-acrylamide concentrations, so a variety of gels were made. An atomic force microscope was calibrated and then used to find the elastic moduli of different polyacrylamide gels, both in the same manner documented by Thomas et *al.*[32] The cantilever used had a force constant of 0.06 to 0.1 N/m. The indentation was performed with an approach velocity of 10 μm/s and a maximum deflection of 50 nm. The force curves were fitted to the Hertz model in order to determine the elastic moduli of the gels. All measurements were made at room temperature. For the cell traction force experiment documented in this paper, an 8% acrylamide/.1% bis-acrylamide gel was produced, which according to our measurements had an elastic modulus of about 7.5 kPa.
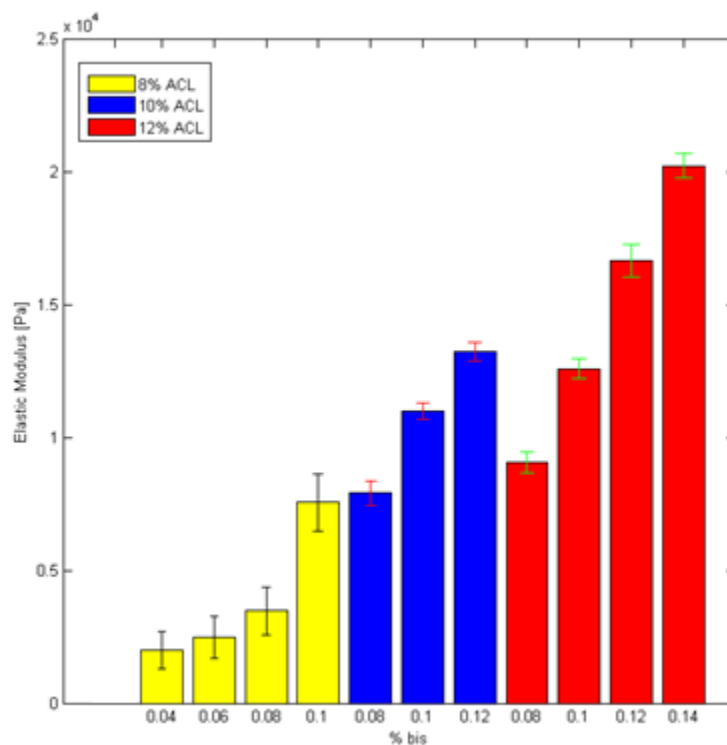
Figure 7: Elastic moduli of polyacrylamide gels with varying polymer/crosslinker ratios [32]. The condition used for this experiment was 8% acrylamide/0.1% bis-acrylamide.

2.11. Collagen Coating

A solution was made using 1 mg of sulfo-SANPAH (GBiosciences®), 8 microliters of dimethyl siloxide (Amresco®), and 1000 microliters of HEPES. Buffer was aspirated from the gels and 250 microliters of sulfo-SANPAH solution was pipetted onto each gel. The gels were left in a sterile hood with UV light shining on them for 10 minutes in order to bind the sulfo-SANPAH to the gel surfaces. The gels were then rinsed with HEPES buffer 5 times in order to remove any excess sulfo-SANPAH. Next, a 0.1 mg/mL rat tail collagen (BD Biosciences) solution was prepared in HEPES buffer and 50 microliters of the solution were pipetted onto each gel. The collagen was allowed to settle on the gel surfaces for 1 hour. After this time, the gels were once again rinsed with HEPES buffer 5 times in order to remove excess collagen, and then were submerged in HEPES and stored in a refrigerator until cells were ready to be seeded on the gels.

2.12. Cell Traction Force Imaging

After cells were seeded and starved on gels, every four hours a set of images was taken of each cell. First, a phase image was taken of the cell itself. Next, a fluorescent image was taken of the microbeads under the cell. Each cell's position was recorded in terms of its location over the grid at the bottom of the gel, and position information was updated after each imaging session. The experiment was ended when one full cell cycle had completed. After this point, the medium in the petri dish was aspirated and replaced by PBS. After a few minutes, the PBS was aspirated and 0.25% trypsin was introduced to the dish in order to remove the cells from the gel surface. At this time, new fluorescent images were taken to match the positions of each previously acquired fluorescent image. The positions of these images were pinpointed using the recorded cell location information as well as by searching for bead artifacts from the original fluorescent images.
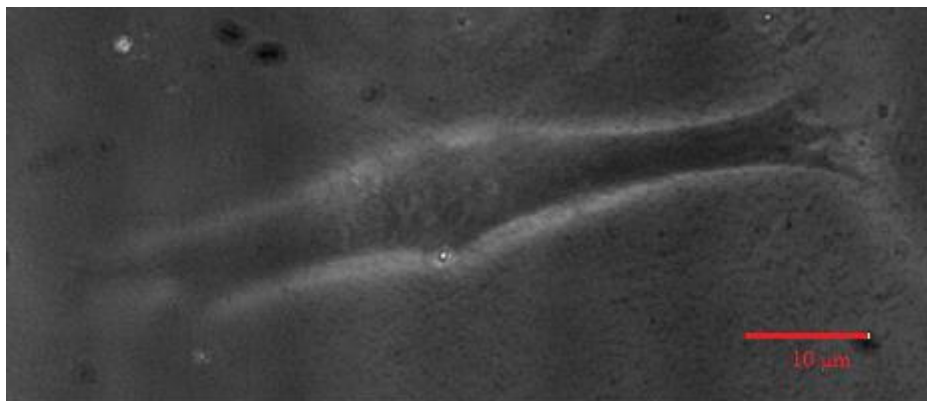
Figure 8: Phase image of first cell sampled at 40x magnification.

2.13. Exclusion Criteria

Cells were excluded from selection for cell traction force experiments for a variety of reasons. First, the cell had to appear healthy. This was gauged by the cells' phenotypes. Rounded cells were generally not selected for study, but elongated cells were considered favorable. Next, the cells had to be at least somewhat isolated.

Cells that were in direct contact with other cells could not be used, as this would cause the cell to exert much more force[10] and it would be impossible to attribute all measured forces to the selected cell. Additionally, cells that were less than a cell length from a neighbor were typically not selected either, because the neighboring cell could mitigate or contribute to the force magnitudes measured, and furthermore because the chances of such a cell migrating into contact with its neighbor after a short period of time was very likely. Finally, cells that were too isolated were not sampled either. If a cell is very far from any neighboring cells, there is a strong likelihood that the cell's health may deteriorate over the course of the experiment, sometimes leading to cell death. Besides the fact that cells support one another, the absence of cells in an area could also indicate a region that did not receive an adequate collagen coating.

Once an ideal cell is found, it can still be excluded. If the beads underneath the cell are not ideal, it cannot be used in the experiment. Examples of this include the presence of large aggregates of beads that make normal-sized beads hard to detect later on during image analysis, or regions of low bead density that will not provide sufficient displacement data. Next, if the cell, during the course of the experiment, comes into direct contact with another cell, dies, or appears to not be synchronized with the rest of the cells (early or late cell division), it will be excluded.

2.14. Image Drift Removal

Before a displacement field could be calculated showing the displacements of beads, the fluorescent images had to be checked for drift and the images had to be cropped and realigned accordingly. The term "drift" refers to any accidental displacement or misalignment of the petri dish between the time a cell image was taken and the time when a corresponding image was taken after the application of trypsin. In MATLAB®, four regions were selected from the stacked images. Usually the four regions chosen were within the four corners of the stacked images, as these points would be the furthest from the cell, which was usually at the center of the image, and thus it would be unlikely that any displacements measured there would have to do with the cell's traction force. The displacements of all four of these regions were averaged and the stacked images were realigned based on this information. Lastly, a rectangular area around the cell was selected as the region of prime interest. Area outside this region was cropped out in order to reduce the computational workload within the next steps of the experiment, as well as to limit the influence of any neighboring cells on traction force analysis.

2.15. Displacement Field Generation

After the images were properly cropped and aligned to account for drift, bead displacements were tracked by Particle Image Velocimetry (PIV) in MATLAB® with a function called "mpiv".[31] A vector field displaying all the displacements along the area selected was produced. Next, the border of the cell was outlined. With the outline of the cell on top of the displacement vector field, the vectors could be analyzed visually for validity. Typically, the displacements should be at their maximum around the leading and rear edges and be directed towards the center of the cell. Furthermore, the displacements under the center/nucleus of the cell should be nearly zero or very small. Images that did not follow these trends were reanalyzed. If the reanalyzed images still did not make sense, the initial images were investigated to see if a neighboring cell was skewing the data or if an error had been made during image acquisition.
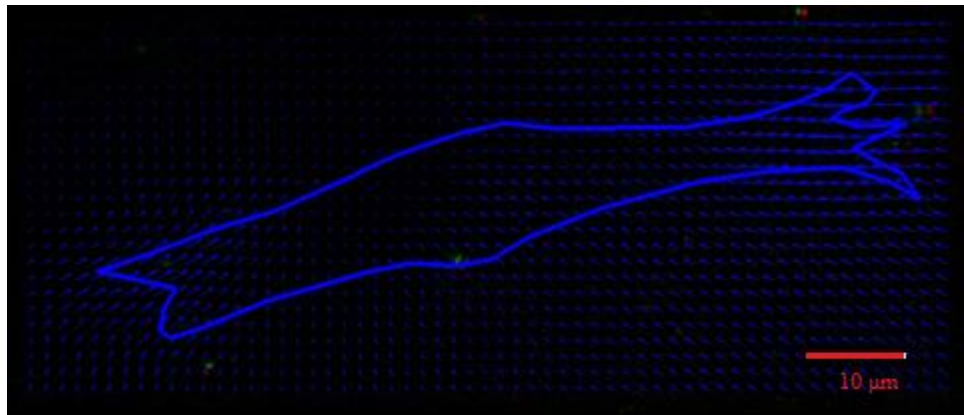
Figure 9: Displacement field generated for first cell sampled. Vectors with the greatest intensity are usually located at the ends of the major filopodia, as seen here.

2.16. Finite Element Analysis of Substrate Surface

Because the gel used was 8% acrylamide and 0.1% bis-acrylamide, the stiffness utilized in stress and force calculations was 7.5 kPa. The gel was approximately 100 micrometers thick, which was calculated by dividing the volume of polyacrylamide solution used, 64 µL, by the area of the glass slide the gel was formed on, which was 625 mm^2. Polyacrylamide gel is known to be an isotropic and elastic material with a Poisson's ratio of about 0.4.

Using ANSYS (ANSYS® Inc.), a finite element analysis software, the substrate surface of each set of images was modelled in three dimensions, taking into account the gel's thickness. Bead displacement vectors were mapped onto the surface of the model. Next, the surface of the substrate was separated into an array of 16 x 16 pixel squares, about .416 µm^2, so that each square region could be analyzed independently of the surface as a whole. Each grid square was referred to as a "node" and each nodal displacement was determined by averaging the

displacements of all beads located on a given node. The only fixed boundary condition was the bottom of the gel, as it was attached to the glass slide. Because the substrate was in force equilibrium,

$$[K]\{u\} = \{F\}$$

where [K] represents the global stiffness matrix, {u} is a nodal displacement vector, and {F} is the nodal force vector. All nodes outside of the previously designated cell boundary specified during displacement field generation had their forces set to zero in order to minimize the influence of neighboring cells or any other potential source of error. Solving this equation for each node gave us F_i, the force at each node, where "i" is the node index.

From the force data, shear stress was calculated using the following equation,

$$F_i = S_i \times da$$

where "da" is the element area, referring to the 16 x 16 pixel area. After completion of finite element analysis, the stresses were plotted in an intensity map to show where the greatest stresses were applied under the cell. The forces and stresses at each point were summed, with the force sum used as the total traction force magnitude of that particular cell.

$$S_{Total} = \sum_{i=1}^{n} S_i \quad , \qquad F_{Total} = \sum_{i=1}^{n} F_i$$
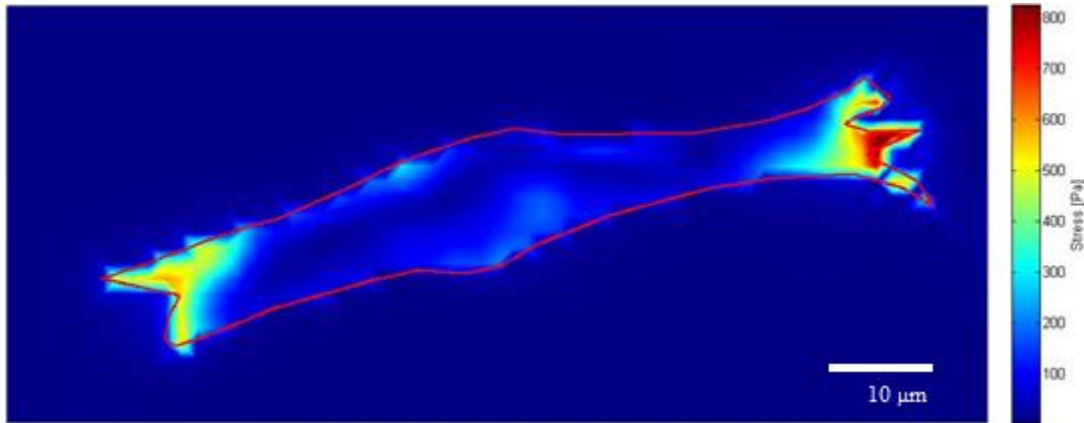
Figure 10: Stress map of first cell sampled. The greatest stresses are observed at the leading and trailing edges of the cell.

MATLAB® also calculated the area within the specified cell boundary, which was used as the spreading area of each cell, as well as the perimeter of cell border. Besides acquiring spreading area data, the area and perimeter were used to calculate the circularity of each cell. Major and minor axis lengths were later measured in ImageJ in order to calculate the elongation index.

While we typically report our findings in terms of total traction force, other studies have reported average force applied to a post[29], total traction stress[30], or even traction stress as a percentage of the maximum reported value[25]. One downside to our method and choice of data reporting is that a noise signal or positional error can propagate along the entire surface of the gel. In this instance, reporting the total traction force of a cell may increase the variance between cells of varying size, as large cells will be more affected by noise or error than a small cell would, due to it having more nodes.

2.17. Statistical Methods

After compiling traction force data, average forces were calculated for each time point and cell phase. Using the Microsoft® Excel "Analysis Toolpak" add-in, an ANOVA (analysis of variance) was performed for data grouped by time point and by phase, along with a statistical power analysis for each ANOVA. A multivariable linear regression that incorporated spreading area, circularity, and cell phase was performed through the MATLAB® "fitlm" command.

Minimum error was estimated by the smallest fluctuation measured by any cell between two consecutive time points that fell within the same phase. This happened to be Cell 2 at its 8 and 12 hour time points.

For further analysis, Cell 2 had its traction force reanalyzed at 8 and 12 hours. This time, however, the nucleus was selected as the region of interest instead of the entire cell. Typically, near zero forces are expected to be detected under the cell's nucleus, so any force measured under the nuclei was considered an error.

3. Results

3.1. Staining Results
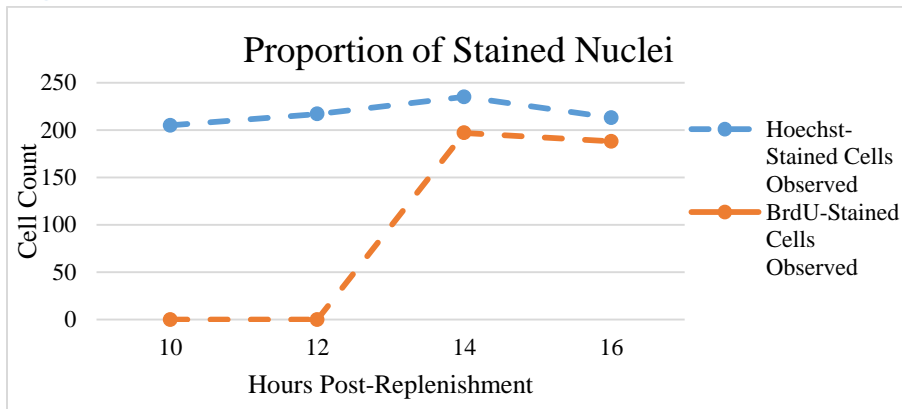
Figure 11: Graph of cells positively-expressing BrdU stain versus cells stained by Hoechst. S phase appears to begin between 12 and 14 hours. A portion of the cellular population did not change phase at this time, suggesting that some of the cells did not re-enter the cell cycle.

For the staining experiments, cells were fixed in 2-hour intervals. For each time point, six images were taken and the number of cells observed in the respective images were summed to characterize cellular activity at each time point. Based on the BrdU versus Hoechst data, the G1/S phase transition occurred between 12 and 14 hours after serum levels were increased. About 10% of cells did not become stained with BrdU although they were stained with Hoechst; this could indicate that these cells were arrested in G0 phase. Based on later time points, cell division occurred between 26 and 28 hours post-replenishment.
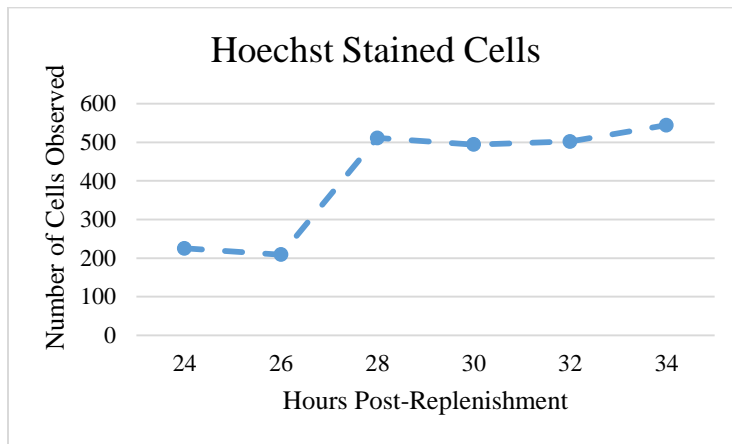
Figure 12: Graph of cells stained for Hoechst around the time of cell division. Cell division appears to take place between 26 and 28 hours.

3.2. Traction Force Results

The following data was collected from a real-time traction force experiment where 9 synchronized cells were tracked over the course of 24 hours.

Force (nN)

Time (Hours)	Cell 1	Cell 2	Cell 3	Cell 4	Cell 5	Cell 6	Cell 7	Cell 8	Cell 9
4	372.0	144.0	178.0	54.0	73.0	55.0	40.0	66.0	64.0
8	437.0	94.0	230.0	105.0	94.0	76.0	46.0	35.0	20.0
12	442.0	96.0	254.0	118.0	86.0	34.0	56.0	66.0	41.0
16	313.0	157.0	236.0	141.0	145.0	86.0	63.0	83.0	22.0
20	330.0	77.0	126.0	72.0	95.0	38.0	52.0	75.0	36.0
24	188.0	57.0	104.0	174.0	180.0	84.0	50.0	123.0	34.0

Table 1: Cell traction force data of each cell at each time point. Data rounded to the nearest whole nN.
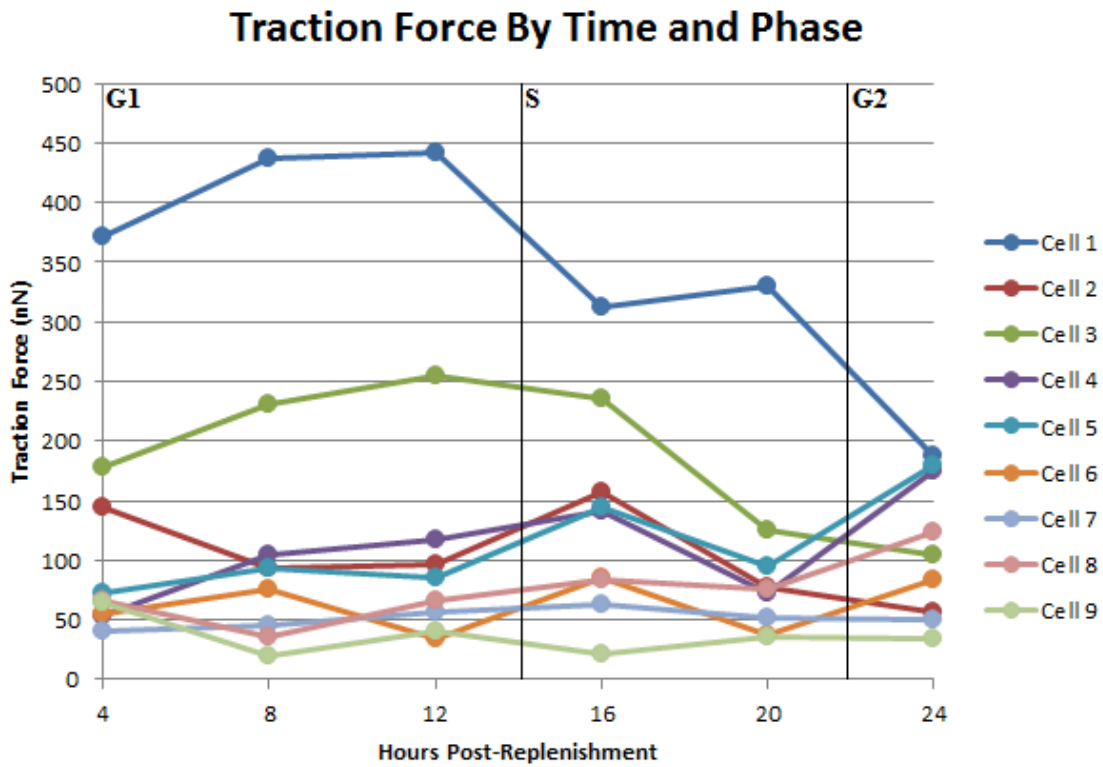
Figure 13: Graphical representation of cell traction forces for each individual cell over the span of 24 hours. It is clear that Cell 1 and possibly Cell 3 are outliers.

29
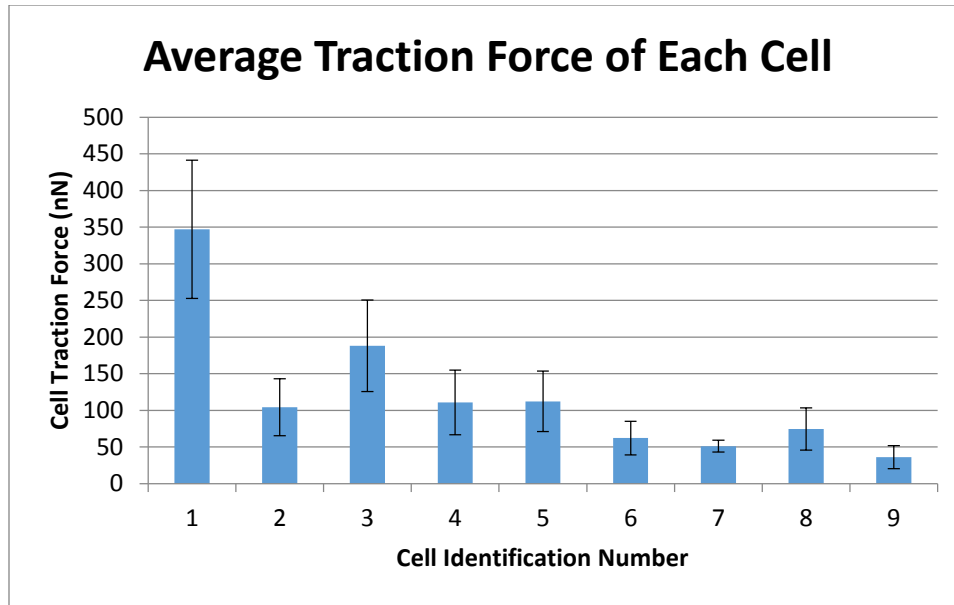
Figure 14: Average cell traction force for each cell with standard deviation plotted as error bars. Cell 1 is clearly an outlier.

Table of Force (nN) Averages, Variances, and Standard Deviations by Individual Cells								
Cell #	1	2	3	4	5	6	7	8	9
Average	347	104	188	111	112	62.2	51.2	74.7	36.2
Variance	8900	1500	3880	1940	1700	533	63.4	826	253
St. Dev.	94.3	38.8	62.3	44.1	41.3	23.1	7.96	28.7	15.9

Table 2: Table of average forces (nN) of each cell sampled, along with variance and standard deviation. Variance is much higher among the cells exerting more force, as expected.

Because Cell 1 had such massive forces recorded in comparison to the other cells sampled, it should be treated as an outlier. After excluding Cell 1 on the basis of it generating too much force, a Grubbs' test indicated that Cell 3 was an outlier ($p > 0.05$). Both cells were excluded when determining phase and time point traction force averages in order to reduce variation.
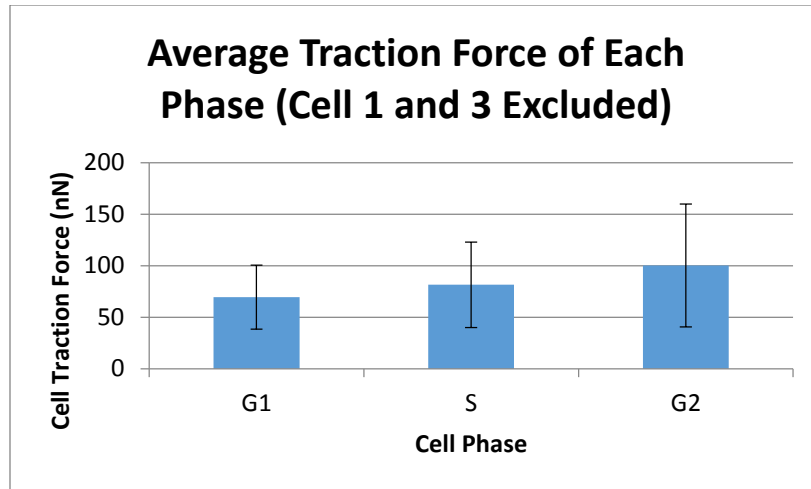
Figure 15: Average cell traction force for each phase with standard deviation plotted as error bars.

Traction Force Data by Phase (Cell 1 and 3 Excluded)			
Phase	G1	S	G2
Average	69.7	81.6	100.3
Variance	961	1720	3560
St. Dev.	31.0	41.5	59.7

Table 3: Table of average forces (nN) of each phase sampled, along with variance and standard deviation.
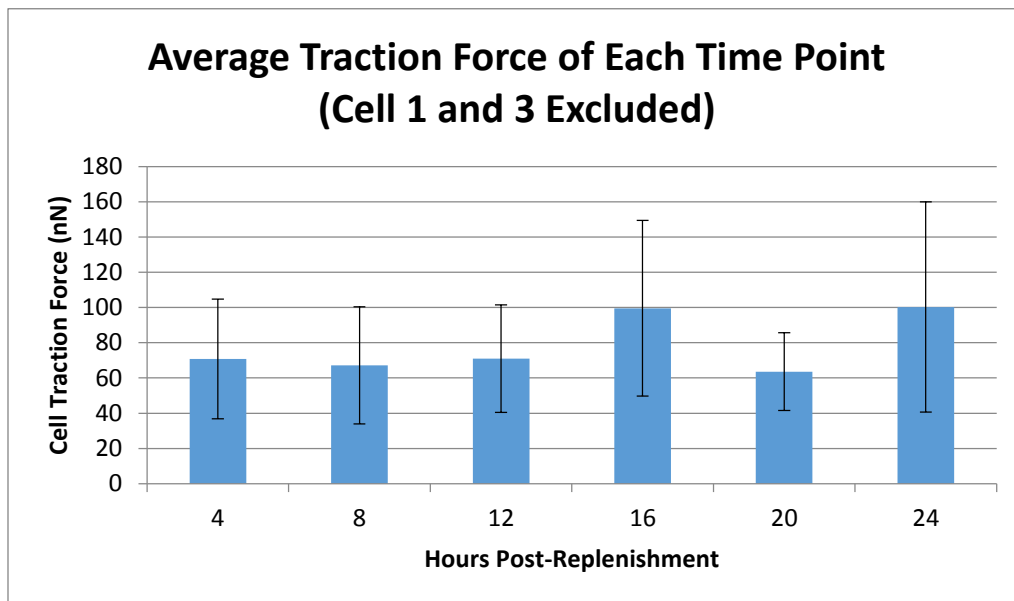
Figure 16: Average force for each time point with standard deviations plotted as error bars. The variation is much more acceptable with the two outliers removed. Two peaks appear on this graph at 16 and 24 hours.

Traction Force Data by Time Point (Cell 1 and 3 Excluded)						
Time	4	8	12	16	20	24
Average	70.9	67.1	71.0	99.6	63.6	100.3
Variance	1150	1110	930.0	2480	486	3560
St. Dev.	33.9	33.3	30.5	49.8	22.1	59.7

Table 4: Table of average forces (nN) of each phase sampled, along with variance and standard deviation.

An ANOVA (analysis of variance) was used for both the cell phase and time point averages to determine if any average was statistically different from another. In both cases, the F value did not exceed the F critical value, so the null hypothesis that all averages are equal could not be rejected. A power analysis of each ANOVA was conducted.

ANOVA of Cell Traction Force Phase Averages

Groups	Count	Sum	Average	Variance		
G1 Phase	21	1463	69.7	961		
S Phase	14	1142	81.6	1720		
G2 Phase	7	702	100.29	3560		
ANOVA						
Source of Variation	SS	df	MS	F	P-value	F crit
Between Groups	5091	2	2550	1.58	.219	3.23
Within Groups	62900	39	1610			
Total	67991	41				

Table 5: Information yielded from ANOVA on average traction forces recorded by phase.

Power Analysis of CTF-Cell Phase ANOVA				
dfB	2		α	0.05
dfE	39		F-crit	3.24
SSB	5090		β	.685
MSE	1610		1-β	.315
n	42			
k	3		Power:	.315
f	.274	Sample Size Required for 80% Power:		132
RMSSE	.336			
λ	3.16			

Table 6: Data involved in acquiring ANOVA power and ideal sample size for CTF-cell phase averages.

ANOVA of Cell Traction Force Time Point Averages

Groups	Count	Sum	Average	Variance		
Hour 4	7	496	70.9	1150		
Hour 8	7	470	67.1	1110		
Hour 12	7	497	71.0	929		
Hour 16	7	697	99.6	2480		
Hour 20	7	445	63.6	486		
Hour 24	7	702	100.3	3560		
ANOVA						
Source of Variation	SS	df	MS	F	P-value	F crit
Between Groups	9690	5	1940	1.12	.330	2.48
Within Groups	58300	36	1620			
Total	67990	41				

Table 7: Information yielded from ANOVA on average traction forces recorded by time point.

Power Analysis of CTF-Time Point ANOVA			
dfB	5	α	.05
dfE	36	F-crit	2.48
SSB	9690	β	.626
MSE	1620	1-β	.374
n	42		
k	6	Power:	.374
f	.377	Sample Size Required for 80% Power:	96
RMSSE	.413		
λ	5.98		

Table 8: Data involved in acquiring ANOVA power and ideal sample size for CTF-time point averages.

Another way to deal with the outliers is to reduce their impact by normalizing all the data to the initial traction force readings for each cell. The cells designated as outliers can be left in for this type of analysis, because their large force magnitudes will not necessarily produce a great deal of variance in this setting. To normalize the data, each force reading was divided by the initial 4 hour reading for that cell. When performing ANOVAs on this data, the 4 hour readings were not included since they are all equal to 1.
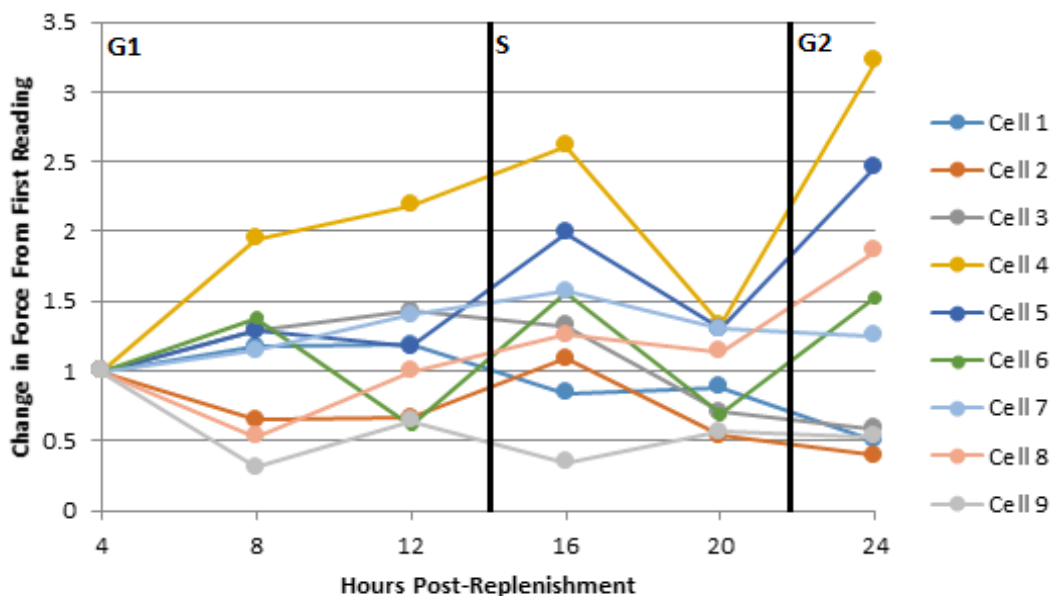
Figure 17: Graphical representation of the respective changes in cell traction force starting at 4 hours over the span of 24 hours, with cell phase transitions marked.

Table of Normalized Force Averages, Variances, and Standard Deviations by Individual Cells								
Cell #	1	2	3	4	5	6	7	8	9
Average	.919	.668	1.07	2.26	1.64	1.16	1.34	1.16	.478
Variance	.079	.068	.152	.503	.313	.215	.026	.232	.020
St. Dev.	.281	.260	.390	.709	.560	.464	.162	.481	.143

Table 9: Table of average forces (nN) of each cell sampled, along with variance and standard deviation. Variance is much higher among the cells exerting more force, as expected.
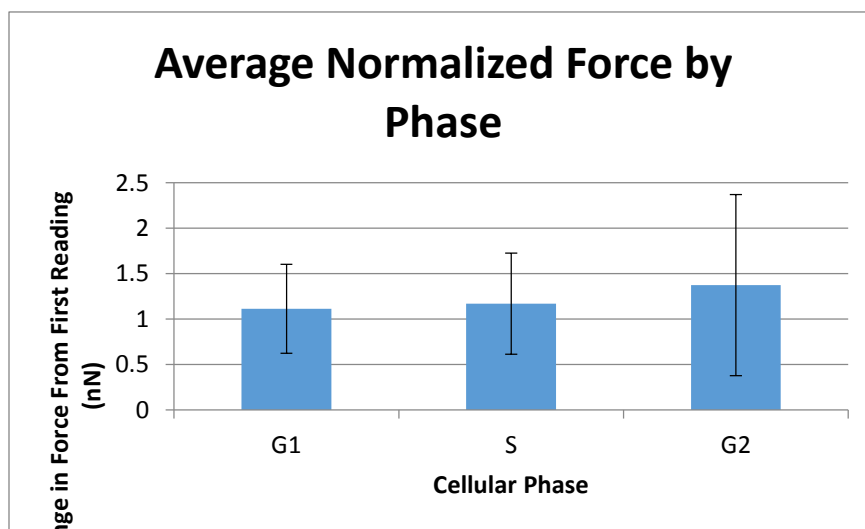
Figure 18: Average change in cell traction force from the 4-hour reading for each phase, with standard deviation plotted as error bars.

Normalized Traction Force Data by Phase			
	G1	S	G2
Average	1.11	1.17	1.37
Variance	.238	.309	.991
St. Dev.	.488	.556	.996

Table 10: Table of average normalized forces of each phase sampled, along with variance and standard deviation.
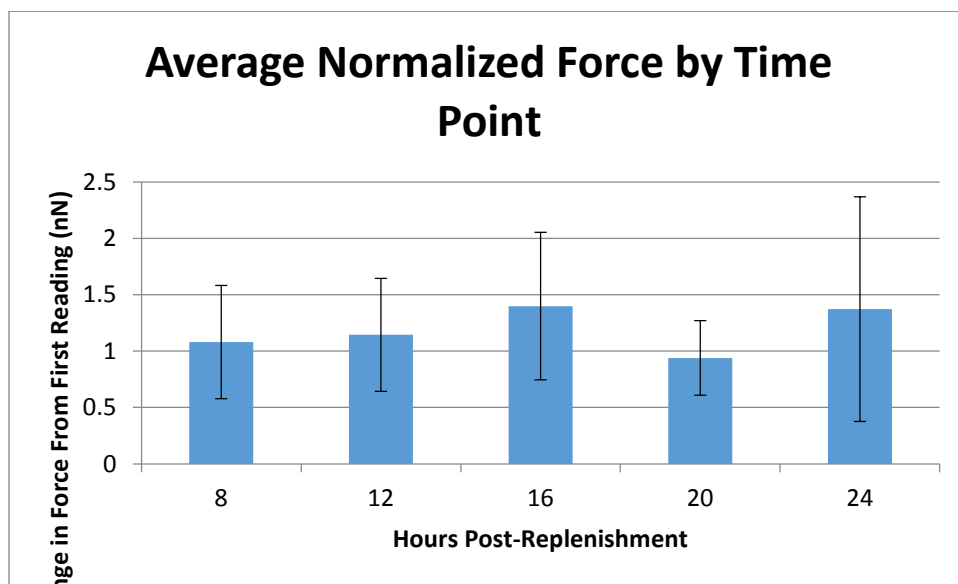
Figure 19: Average change in cell traction force from the four hour reading for each time point, with standard deviation plotted as error bars.

Normalized Traction Force Data by Time Point					
Time Point	8 Hours	12 Hours	16 Hours	20 Hours	24 Hours
Average	1.08	1.14	1.40	.939	1.37
Variance	.252	.251	.427	.110	.991
St. Dev.	.502	.501	.654	.331	.996

Table 11: Table of average normalized forces of each time point sampled, along with variance and standard deviation.

ANOVA of Normalized Cell Traction Force Phase Averages

Groups	Count	Sum	Average	Variance		
G1 Phase	18	20.0	1.11	.235		
S Phase	18	21.0	1.17	.307		
G2 Phase	9	12.3	1.37	.986		
ANOVA						
Source of Variation	SS	df	MS	F	P-value	F crit
Between Groups	.408	2	.204	.502	.609	3.22
Within Groups	17.1	42	.407			
Total	17.5	44				

Table 12: Information yielded from ANOVA of average normalized traction force recorded by phase.

Power Analysis of Normalized CTF-Phase ANOVA			
dfB	2	α	0.05
dfE	42	F-crit	3.22
SSB	.408	β	.873
MSE	.407	1-β	.127
n	45		
k	3	Power	.127
f	.149	Sample Size Required for 80% Power	435
RMSSE	.183		
λ	1.00		

Table 13: Data involved in acquiring ANOVA power and ideal sample size for normalized CTF-cell phase averages.

ANOVA of Normalized Cell Traction Force Time Point Averages

Groups	Count	Sum	Average	Variance		
8 Hour	9	9.71	1.08	.250		
12 Hour	9	10.30	1.14	.247		
16 Hour	9	12.6	1.40	.425		
20 Hour	9	8.45	.939	.109		
24 Hour	9	12.3	1.37	.986		
ANOVA						
Source of Variation	SS	df	MS	F	P-value	F crit
Between Groups	1.38	4	.344	.854	.500	2.61
Within Groups	16.1	40	.403			
Total	17.5	44				

Table 14: Information yielded from ANOVA of average normalized traction force recorded by time point.

Power Analysis of Normalized CTF-Time Point ANOVA			
dfB	4	α	.05
dfE	40	F-crit	2.61
SSB	1.38	β	.753
MSE	.403	1-β	.247
n	45		
k	5	Power	.247
f	.275	Sample Size Required for 80% Power	165
RMSSE	.308		
λ	3.41		

Table 15: Data involved in acquiring ANOVA power and ideal sample size for normalized CTF-time point averages.

In terms of statistical power, the non-normalized data is much stronger. However, the normalized data allows for the inclusion of the two outlier cells in statistical analysis and additionally makes for a better graphical representation of force fluctuations by removing the visual bias of large and small starting magnitudes.

In both cases, the time point data had greater statistical power than cell phase data. In the case of the non-normalized data, the power of the cell phase ANOVA was 31.5% whereas the

time point ANOVA was 37.4%. The sample size was 42 readings (7 cells at 6 time points), but to reach a statistical power of approximately 80% for the cell phase averages, we would need a sample size of 132, while for the time point averages, we would need a sample size of 96. The reason the time point averages have greater statistical power is because, at least in the case of S phase, we see a major fluctuation in traction force experienced by the majority of the cells sampled. This fluctuation occurs at 16 and 20 hours, both of which are categorized as being in S phase. At 16 hours, we see a large increase in traction force, along with an expected increase in variation. At 20 hours, however, the forces and variation reduce back to a magnitude that is very similar to how the cells acted in G1 phase.

Considering that, of the four ANOVAs presented, the higest statistical power was 37.3%, while ideally the power should be 80% or higher, confidence in the null hypothesis being true is very low based on this data. With larger sample sizes, a more definite conclusion could be made from an ANOVA.

3.3.   Cell Traction Force Error Analysis

Cell 2 had a total traction force measurement of 94 nN at 8 hours and 96 nN at 12 hours, meaning it only fluctuated by 2 nN in this time. This was the smallest recorded fluctuation between two consecutive time points falling within the same cell phase, so 2 nN was considered to be the minimum error.

The nucleus of Cell 2 at 8 hours was analyzed independently of the cell and was found to have a total traction force of about 3 nN. Since the traction force measured under a cell's nucleus should be close to zero, this force was assumed to be error. The nucleus of Cell 2 at 12 hours was analyzed in the same manner. Though the cell had changed shape and migrated from its previous location, traction force under the nucleus was again measured to be about 3 nN, which suggests that the error applied to each set of images may be somewhat uniform or that these similar readings may be caused by the resolution of our analytical method. To test this, several other time points were tested from other cells of similar size and traction force magnitude to Cell 2, and all nuclei measured for total traction force were in the range of 2-4 nN.

3.4.   Cell Spreading Area Results

Area (µm^2)

Time (Hours)	Cell 1	Cell 2	Cell 3	Cell 4	Cell 5	Cell 6	Cell 7	Cell 8	Cell 9
4	1740.0	1064.0	808.0	529.0	720.0	763.0	677.0	868.0	626.0
8	1924.0	627.0	1371.0	909.0	905.0	940.0	731.0	753.0	561.0
12	1683.0	747.0	1614.0	876.0	1037.0	682.0	788.0	1260.0	898.0
16	1589.0	1209.0	1263.0	1332.0	1498.0	1343.0	1150.0	1435.0	405.0
20	1429.0	833.0	985.0	1123.0	1091.0	874.0	907.0	1574.0	770.0
24	1318.0	713.0	887.0	1426.0	1478.0	1551.0	818.0	1654.0	1482.0

Table 16: Cell spreading area data for each cell at each time point. Data rounded to the nearest whole µm^2.
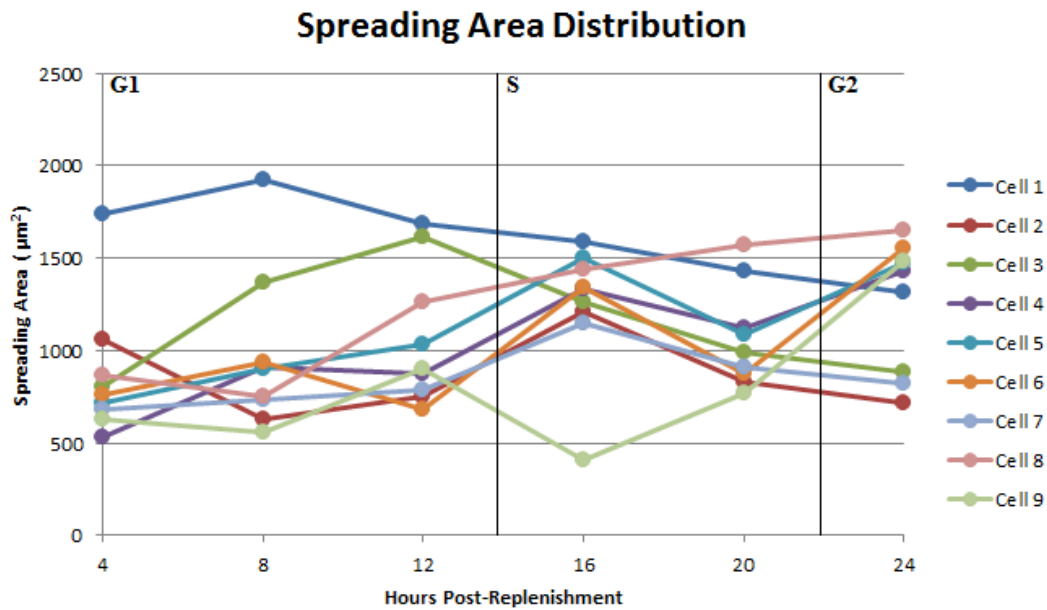
Figure 20: Graphical representation of cell spreading area for each individual cell over the span of 24 hours.

3.5. Cellular Circularity Results

Time (Hours)	Cell 1	Cell 2	Cell 3	Cell 4	Cell 5	Cell 6	Cell 7	Cell 8	Cell 9
4	.181	.292	.210	.292	.257	.274	.356	.308	.184
8	.187	.404	.098	.308	.237	.130	.215	.205	.271
12	.183	.203	.076	.145	.243	.293	.215	.162	.219
16	.167	.190	.130	.146	.220	.250	.317	.170	.331
20	.154	.167	.172	.270	.246	.251	.317	.262	.344
24	.144	.147	.126	.205	.240	.248	.337	.266	.524

Table 17: Circularity for each cell at each time point.
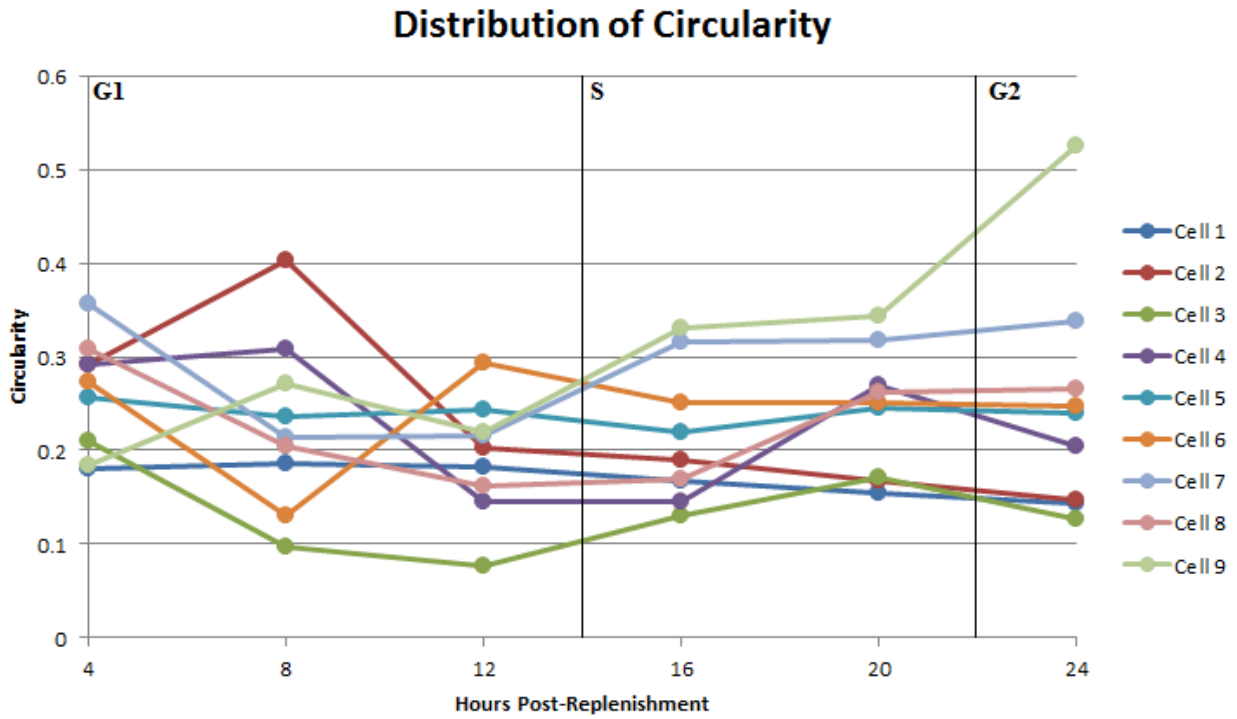
Figure 21: Graphical representation of circularity for each individual cell over the span of 24 hours.

3.6. Cellular Elongation Index Results

Elongation Index

Time (Hours)	Cell 1	Cell 2	Cell 3	Cell 4	Cell 5	Cell 6	Cell 7	Cell 8	Cell 9
4	6.37	6.51	10.4	4.81	7.23	7.04	3.81	5.74	5.94
8	9.32	2.78	17.4	3.61	7.53	8.49	7.47	7.51	5.70
12	8.45	7.99	23.6	8.62	7.90	5.07	5.31	6.61	3.06
16	9.61	9.76	7.76	8.79	9.49	5.74	4.21	8.46	4.52
20	9.30	7.12	8.82	8.51	8.30	7.50	3.84	6.62	3.14
24	10.1	9.21	13.5	9.53	5.33	3.86	3.94	8.70	2.71

Table 18: Elongation index for each cell at each time point.
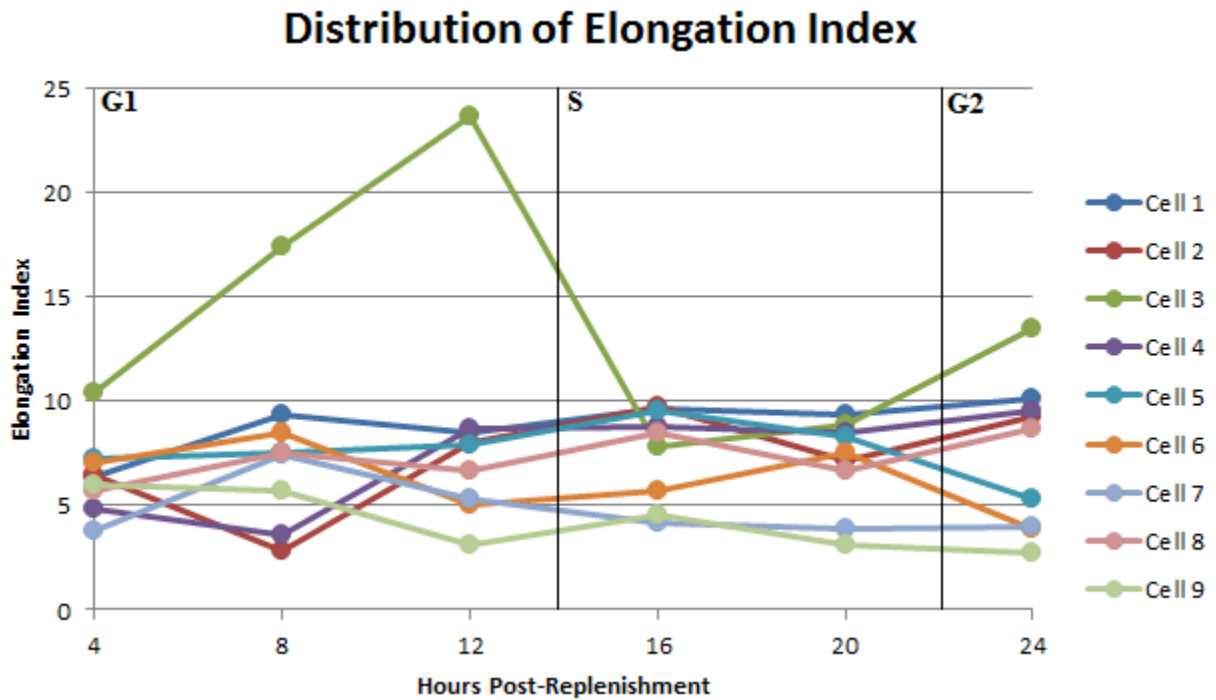
Figure 22: Graphical representation of elongation index for each individual cell over the span of 24 hours.

3.7. Linear Regression

Because the sample size of the data collected was not large enough to make a robust conclusion via an ANOVA, other options were explored. It has been documented that cell spreading area and shape influence traction force,[9,10] and since they had been recorded in this experiment, a linear regression was performed to discover the relationship between force and the other variables recorded.

The regression incorporated cell phase, which was treated as a modifying coefficient on the factors known to contribute to traction force. It was decided that elongation index and circularity would not be included within the same regression, as they are co-dependent. After performing two regressions, it was found that using circularity yielded better p-values than elongation index.

Phase-Based Linear Regression			
Force =1 + SpreadingArea*Phase + Circularity*Phase			
Estimated Coefficients:			
	Estimate	SE	tStat	pValue
Intercept	-28.6	50.1	-.571	.572
SpreadingArea	.096	.041	2.34	.026
Circularity	85.0	107	.796	.432
Phase_G2	86.5	69.4	1.25	.221
Phase_S	136	79.7	1.70	.098
SpreadingArea:Phase_G2	.006	.053	.109	.914
SpreadingArea:Phase_S	-.044	.051	-.862	.395
Circularity:Phase_G2	-404	149	-2.71	.011
Circularity:Phase_S	-419	185	-2.27	.030
Number of observations: 42, Error degrees of freedom: 33			
Root Mean Squared Error: 30.1			
R-squared: .56, Adjusted R-Squared .453			
F-statistic vs. constant model: 5.25, p-value = .0003			

Table 19: Results of linear regression of force as a function of cell phase, spreading area, and circularity.

Based on the regression, spreading area is a reliable contributor to traction force generation. In S phase, it appears to have a reduced contribution, but this coefficient is not necessarily trustworthy due to a high p-value. Circularity is more of an influencing factor for traction force in S phase and G2 phase than in G1 phase. Not much else can be concluded from the regression due to the statistical weakness of certain coefficients.

3.8.   CTF Data from Previous Experiments and Literature

Prior to acquiring the data presented in this paper, our lab had acquired other traction force and spreading area data for 3T3 fibroblasts on gels of varying stiffness with several

different types of ligand coating. These cells were not synchronized and only one CTF measurement was made per cell. More cells were sampled, but much more data was actually collected in the new experiment due to having six time points for every cell. Additionally, the cells sampled in the older experiments were seeded on more than one gel. This greatly increases the chances of stiffness errors. As seen in Figure 6, a given gel condition can have a range of actual stiffnesses that differ from the purported stiffness.
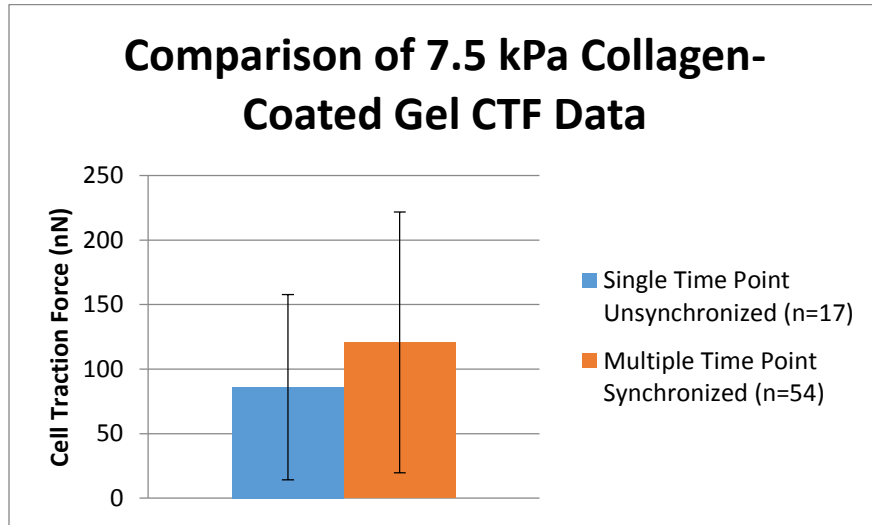
Figure 23: Averages and standard deviations of all data collected from cells on 7.5 kPa collagen-coated gels. No outliers were excluded in the presentation of this data.

Comparison of 7.5 kPa Gel Stiffness Data		
	New Data	Old Data
Average	121	86.0
Variance	10200	5160
St. Dev.	101	72.0

Table 20: Comparison of old data (specifically the data from 7.5 kPa stiffness gels) to the newly acquired data presented in this paper. While average forces observed were slightly higher, variance was much higher. Respective sample sizes were 54 (new) and 17 (old).
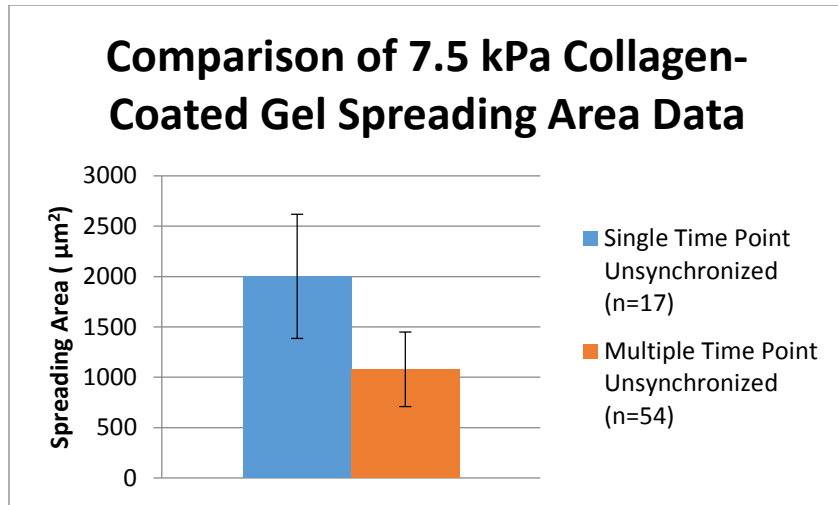
Figure 24: Averages and standard deviations of all data collected from cells on 7.5 kPa collagen-coated gels. No outliers were excluded in the presentation of this data.

Besides comparing our new data to old data, we compared it to data from literature published by other labs. Lemmon *et al.* used a system of deformable cantilever posts to measure the traction force of NIH3T3 fibroblasts over the span of 24 hours.[29]
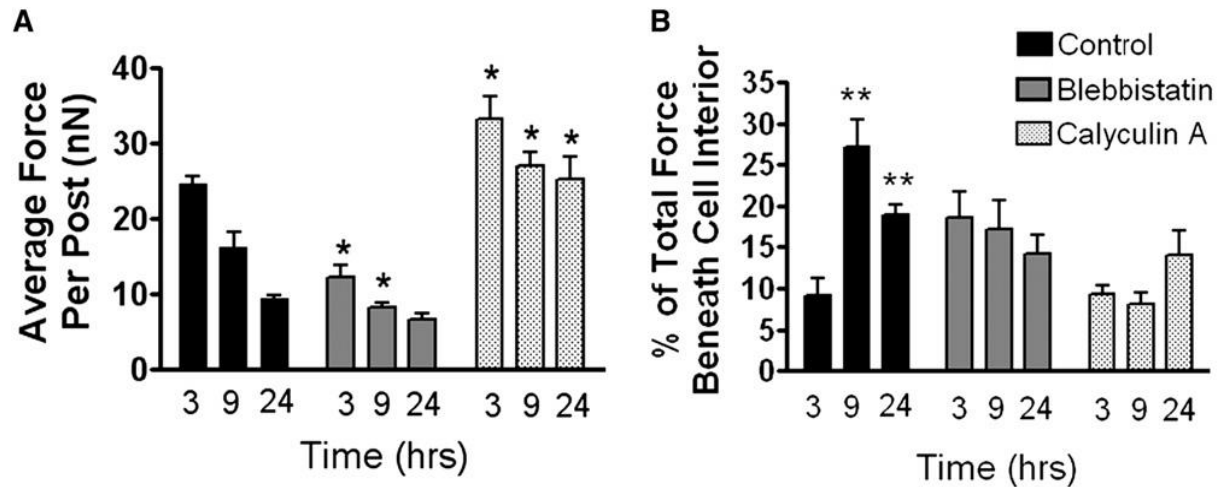
Figure 25: Graphs of some results taken from Lemmon *et al.* The data portrayed by the black columns (control) are of key relevance, as they were untreated 3T3 fibroblasts [29].

Another paper that compiled 3T3 fibroblast traction results was Munevar *et al.* Rather than reporting traction force values, they reported traction stress values. As such, our stress data was used in place of force data for a comparison.

TABLE 1 Average traction stress for migrating normal NIH 3T3 and H-ras transformed fibroblasts

Cell number	Average traction stress (dyn/cm²)	
	3T3	Pap2
1	1.07×10^4	1.43×10^4
2	1.81×10^4	7.80×10^3
3	2.67×10^4	9.95×10^3
4	4.17×10^4	7.81×10^3
5	3.69×10^4	
6	8.08×10^4	
7	2.21×10^4	
8	1.67×10^4	
9	1.94×10^4	
Mean	3.03×10^4	9.97×10^3
SD	2.13×10^4	3.06×10^3

Table 21: Table from Munevar *et al.* comparing 3T3 and H-4as transformed traction stresses [30].

Comparison of Stress (dyne/cm²) Data		
	Our Data	Munevar *et al.*
Average	10400	30300
Variance	326×10^5	455×10^6
St. Dev.	5710	21300

Table 22: Comparison of stress data between our results and those of Munevar *et al.* [30]
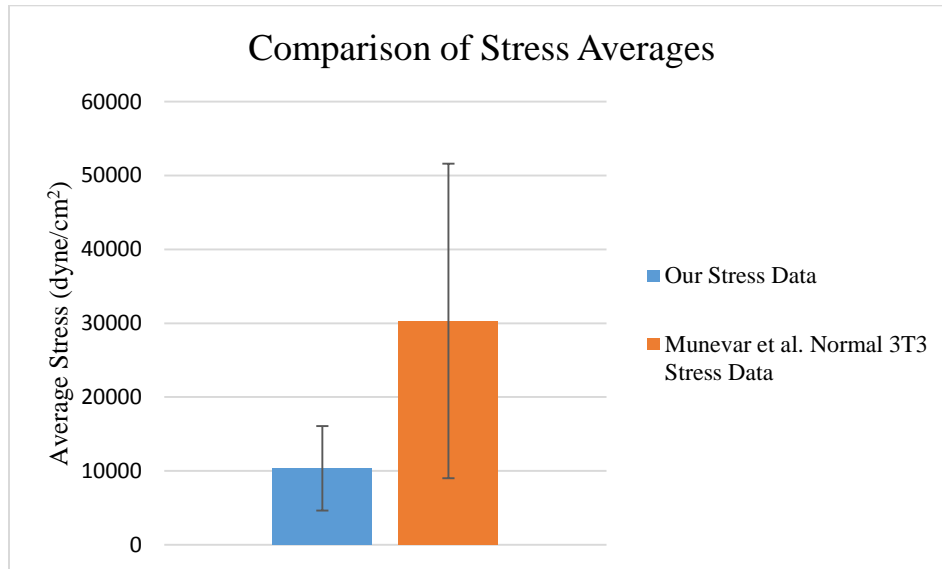
Figure 26: Comparison of traction stress averages and standard deviations between the data presented in this paper and the data from Munevar *et al.* [30]

4. Discussions

4.1. Cell Phase's Influence on Traction Force

Overall, there was very little indication of any trend between cell phase and cellular traction force. While force averages did tend to increase with each successive phase, variation did as well. The cells with larger spreading areas tended to have greater force averages and variations than smaller cells.

Based on the ANOVAs, it is clear that we cannot prove any statistically significant difference between traction force averages within the different phases, or even at different time points. The linear regression produced had a fairly low accuracy. From it, we can conclude that spreading area plays a large role in determining total traction force magnitude, but its influence does not change much through the phases. Additionally, circularity seems to influence total traction force more during S phase and G2 phase than in G1 phase.

While there was no statistically significant indicator that cell phase influences traction force generation, there were some interesting trends with regards to force fluctuations. At the 16 and 24 hour time points, the average traction force was higher than other time points. Reviewing the original (Figure 13) and normalized (Figure 17) data, we see that 7 of the 9 cells sampled increased in force at 16 hours. The exact same 7 cells then had reduced traction force at hour 20. The cells that were not in agreement were Cell 1 and Cell 9, which had the highest and lowest average forces respectively. At hour 24, 6 cells decreased in force while 3 increased. The magnitudes of the decreases in force were very small, while the increases in force were quite large, which led to this time point having a higher average than the previous time point.

Overall, the most interesting piece of information to be taken away is that forces seem to fluctuate within S phase for the majority of cells sampled, initially rising near the start of the phase and then falling back down to roughly the same forces observed in G1 phase.

4.2. Potential Sources of Error

Our findings suggested that a small amount of force (~2-4 nN) was detected under each nucleus of each cell. Nuclei are expected to have nearly zero force applied underneath them. Additional nuclei were sampled and, because we repeatedly found values ranging from 2 nN to 4 nN for each nucleus, it is possible that this is simply the lowest value our methods can yield for an area of this size. If this is not the case, however, these measurements could represent an erroneous transformation of the gel surface, such as from the misalignment of bead images. Such an error would, however, be mitigated through the directionality and magnitude of the actual forces applied by the cell at its edges. Another important distinction to make is that, regardless of which way this error is modelled, it cannot decrease the forces measured, only increase them. Thus, we could say with confidence that error occurring at the nucleus of each cell contributes about 4 nN of its total traction force. This error may be greater for cells with larger nuclei, such as Cell 1.

Another issue was our ability to maintain a constant temperature. The gels were kept in an incubator for most of the experiment at 37° C in order to keep the cells healthy. However, every 4 hours when they were imaged on the microscope, they exposed to room temperature

($\sim$20° C) for about 10-15 minutes. It is unknown how much the temperature was reduced within the dish during this time.

If the gel experienced a loss in temperature, its stiffness would have decreased slightly.[21] It is worth noting that the chart in Figure 6 displays gel stiffnesses at room temperature. This means that, when the gel was taken out of the incubator, the stiffness was initially lower than 7.5 kPa and as the gel approached room temperature, the stiffness would have come closer to this value. Since 7.5 kPa was the stiffness used to calculate force values for every cell at every time point, the cells sampled earlier may have had slightly inflated force values for this reason.
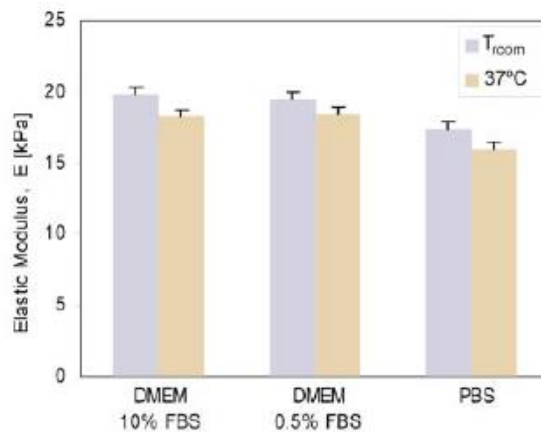
Figure 27: A comparison of polyacrylamide gel stiffnesses at room temperature and 37° C [21].

Besides affecting gel stiffness, temperature may also affect the cytoskeleton of cells. While there is not really any information about how low temperatures might affect cell traction force, it is known that to affect cells negatively in a variety of ways. The length of phases in the cell cycle is increased when culture temperature is lowered, particularly G1 phase.[26] Certain proteins may be denatured or misaggregated, while certain cellular processes like transcription and translation can be slowed or stopped.[27] Considering the range of temperatures the cells experienced while they were on the microscope, they were most likely in a state of moderate hypothermia by the time they were returned to the incubator. While they certainly were able to recover from this shock each time, it is likely that the continuous exposure had some effects.

Lastly, based on Figure 11, about 10% of our starved cells did not re-enter the cell cycle with the rest of the population. Taking this into consideration, it is possible a cell or even a few cells sampled were quiescent or at least re-entered the cell cycle late in comparison to the other cells. While we are not sure of how quiescence could affect traction force generation, this may have complicated data analysis, as potentially one or more cells could have been contributing data to phase averages incorrectly. Another way in which cell phase may have been mischaracterized is by the estimated G2 transition time. The timing was estimated by adding the length of a typical 3T3 fibroblast S phase duration to the S phase transition timing we

determined. A better strategy would have been to use BrdU to detect passage into G2 phase. With a known timing of entry into S phase and an estimate of how long S phase could last, BrdU labelling reagent could be incorporated into a variety of synchronized cultures, each at a different time point. After allowing the cells some time to incorporate the BrdU, they could be fixed. Cells at earlier time points should stain positive for BrdU, while cells at later points would stain negative, indicating that BrdU had been incorporated after S phase had already ended.

4.3.   Comparison to Previously Collected Data

Data collected previously by our lab can be compared to the new data being presented here. While the old data was collected on a variety of gel stiffnesses and surface coatings, the experiment documented in this paper was performed on a 7.5 kPa stiffness gel with a collagen coating, and thus it should only be compared to the data collected for such a condition. The old data is from 3T3 fibroblasts that were not synchronized in any way, and all readings were from separate cells, as they were not tracked for multiple readings of single cells.

One major advantage to real-time traction force experiments is that far more data can be collected. In the previous experiments, 17 cells were sampled, whereas in this experiment only 9 were. However, the sample size for this experiment was 54 because each cell was imaged 6 times. Overall, the synchronized cells seemed to have slightly higher average force with a greater variation than the previous experiments. It is possible that the slightly greater force values recorded in the more recent experiment could be due to the fact that a higher resolution microscope was used for this experiment, and thus the bead displacements acquired may have been more accurately measured.

Interestingly, the old cells analyzed had almost double the average spreading area of the cells studied in the real-time cell tracking experiment. The fact that similar traction forces were observed with vastly different spreading areas indicates a few things. The most likely reason for the low spreading areas observed in this experiment is the serum starvation. When the cells are starved, they complete their current cell cycle and then become arrested in G1/G0. During this time, they are deprived of growth factors. In order for a cell to extend itself across a surface, it must engage in actin polymerization.[22] However, the formation of actin stress fibers and the formation of new focal adhesions is inhibited by the absence of certain proteins and growth factors that can be found in serum.[23] Therefore, most cells during serum starvation will not change their size and shape much until after serum is introduced. While the synchronized cells slowly regain their ability to grow, alter their shape, and migrate, unsynchronized cells are already doing all these things actively.

It is worth noting that the previously recorded data may have suffered from some of the same temperature issues as the experiment presented in this paper. Cells could not remain incubated during imaging and selection of cells took roughly the same amount of time, if not longer due to inexperience, as it did for this experiment. Additionally, the difference in temperature of the gel between when the first and second set of bead images were taken would

have been greater in the previous experiments because, in the experiment documented here, the gel was given time in the incubator to warm up again before trypsin was applied.

4.4.   Comparison to Data from the Literature

In Lemmon *et al.* 3T3 fibroblasts were seeded on an array of deformable cantilevers for traction force measurement. Over the span of 24 hours, it was seen that, while spreading area and overall force increased, the concentration of force on the outer edges of the cells diminished.[29] How cell division was avoided over this time span was not divulged in the paper, but since the cells did not appear to divide over the span of 24 hours, it is possible they used serum starvation as we did for our experiment. The reason they were interested in how the distributions of force changed over time is because they were investigating if the formation of a fibronectin matrix coincided with periods of greater traction force applied around the edges of the cell.

It was found that, over time, while the cells do increase in size, the average traction force applied to each post decreased, which in turn meant that the average amount of force applied at each focal adhesion had most likely decreased.[29] In terms of total traction force, the values did not necessarily change much, as the cells were growing and forming new adhesions on other posts. The best way to compare our results to theirs is to review the stress intensity maps generated for each cell at each time point. Overall, our data agreed with this trend.
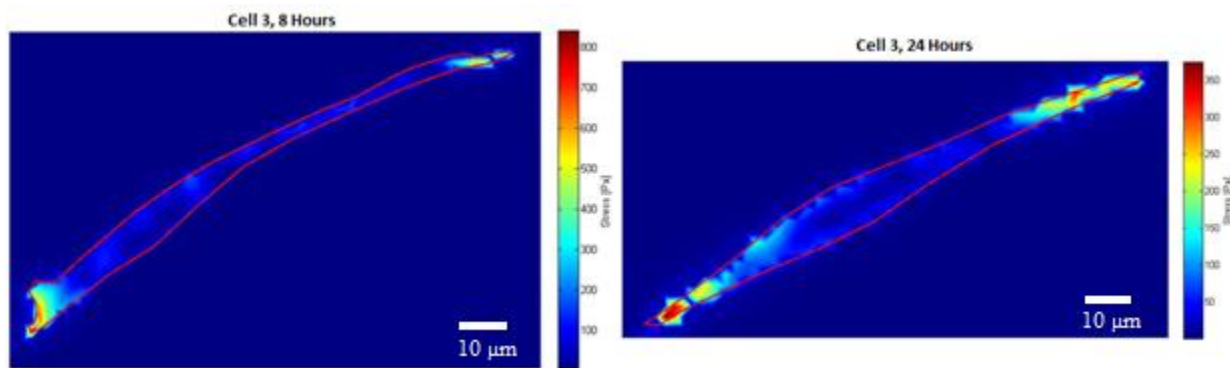
Figure 28: A comparison of two images from our experiment of the same cell at 8 and 24 hours. It is clear that the magnitude of stress at either end of the cell has decreased over time.

Munevar *et al.* also worked with 3T3 fibroblasts on polyacrylamide gels and reported their traction stresses. They were also performing experiments on H-ras transformed 3T3 fibroblasts, but their control group of normal 3T3 fibroblasts is of greater relevance to our experiments. As with our data, there were a few outlier cells. Their overall average traction stress, however, was about three times the magnitude of ours, which may be attributed to our cells undergoing serum starvation and brief periods of hypothermia.
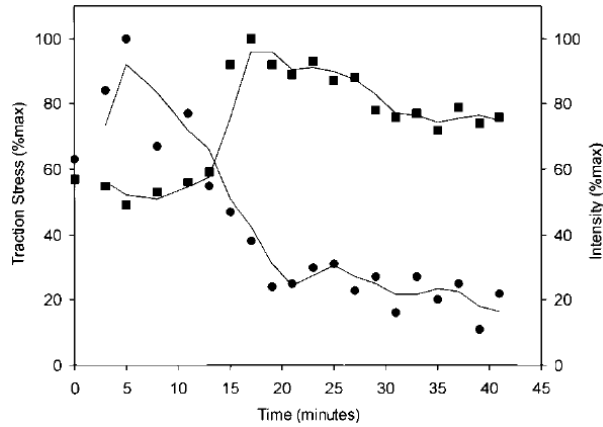
Figure 29: A graph from Beningo *et al.* portraying the traction stress exerted at a single focal adhesion over the span of about 45 minutes. The circles represent traction stress readings, whereas the squares indicate the intensity of a GFP used to detect focal adhesion activity [25].

Beningo *et al.* examined the stresses individual focal adhesions can exert and how they fluctuate over time. In Figure 29, we see about a 75% drop in applied stress within about 15 minutes. This suggests that the four hour time resolution used in our experiment was not ideal, as forces may fluctuate between much shorter time periods. It would seem that ideally multiple images should be taken per hour in order to ensure that peaks are properly detected. However, the focus of our experiment was deciding if cell phase had any effect on traction force, not examining how individual cells' traction force changes over time. If any changes in traction force occurred due to the cells transitioning phases, the effect of individual cells' force fluctuations would be mitigated by the averaging of data sets.

5. Conclusions

Based on all of the work presented here, a few conclusions can be made. First, cell phase has no significant influence on cell traction force. Large force variations caused ANOVAs to be unable to reject a null hypothesis that force averages from different phases and different time points could be equal. The linear model produced did not implicate any significant influence on traction force by cell phase.

Considering that the cells used were all of the same cell type, from the same cell line, seeded on a gel of uniform stiffness with a uniform coating of collagen, and were grown in the same incubator and experimented on in the same fashion, it seems the major differences in their respective traction force averages and variations (shown in Table #3) should be the result of something unique to each individual cell. One possibility is that certain epigenetic traits of the cells affect their traction force generation.

The variability in the data collected may have come from multiple sources. First, cell size and shape varied both on a cell-to-cell basis and with each successive time point. Both of these are contributing factors to a cell's maximum potential traction force, so their variability would likely have influenced the variability of forces measured. Secondly, it is well known that cell traction force fluctuates during cell migration[25], and most of the cells analyzed appeared to be migrating frequently. Lastly, it is possible that temperature changes influenced variations in both this experiment and previous experiments conducted by our lab.

6. Future Recommendations

The findings presented in this paper have generated further questions to be answered. While the experiment documented here suggests that some cells are innately stronger or weaker than others in terms of their ability to generate traction force, we still do not know exactly why this phenomenon occurs.

If this experiment is repeated, the focus should be on S phase. From our force fluctuation data, it appears that, while force does not fluctuate much from phase to phase, most cells fluctuate in a particular way within S phase, starting out higher than G1 and then falling back down to forces similar to G1. If a greater number of readings were taken in S phase and this trend was again observed, this may indicate that a change in cellular mechanics occurs early in S phase.

Any follow-up experiment should ideally be performed on a microscope stand capable of keeping the cells incubated at a proper temperature and gas concentration. Various statistical issues in this experiment were caused by a lack of temperature stability during data sampling. This likely contributed to slight changes in gel thickness, stiffness, cellular activity, and bead layering during analysis. Ideally, all data would be collected in a single experiment as it was in this paper, so that regardless of how close a gel is to its intended stiffness, all data would be offset by the same factor, rather than by a different factor for each gel. Using a microscope that could keep the cells properly incubated would allow for a larger sampling of cells within each experiment, as the dish could stay on the stand indefinitely, much more frequent samplings, and less overall error. Instead of limiting the number of cells in the study and taking images every four hours to minimize exposure to low temperatures, many cells could be sampled and multiple images of each cell could be taken every hour. This would allow for far more data to be collected, and thus more robust conclusions could be made from the experiments.

One test worth performing would be to repeat the experiments documented here, additionally tracking the second generation of cells grown on the gel surface. Traction force data from the parent cell and each daughter cell could be compared to each other to observe how clonal cells may differ in their ability to exert force. For the most part, it would be expected that clonal cells will generate similar forces to one another, but considering the variation generally seen in cell traction force experiments, this will not necessarily be the case.

Another experiment for the future would involve using chemotactic stimulation to motivate cellular migration in a specific direction, then tracking the migrating cells and measuring their traction forces. Having control over the cells' migration patterns would likely mitigate some of the variation we normally see, but more importantly it would allow us to more closely study how traction force relates to cell migration. It would still be a good idea to attain a state of quiescence in the cells beforehand so that cell phase could be factored in if any sudden changes to the rate of migration or traction force magnitudes are noticed. Additionally, it would ensure that each cell could be observed for the maximum amount of time possible.

A logical next step would be to eventually analyze human primary cells with the methods presented in this paper. The most interesting cells to sample would be those involved in wound healing and tissue repair, as traction force arguably has the greatest in vivo significance when utilized in such a manner.

Quiescent cells are commonly found in cell cultures and in live organisms, so it may have been a mistake not to have identified some quiescent cells in this experiment and measured their forces just to have some idea of how being quiescent might affect a cell's traction force. Going forward, it would be an interesting endeavor to try to identify and then study quiescent cells.

Additionally, it would be a good idea to try using alternative techniques to achieve synchronization. Ideally a synchronization technique that did not result in quiescence could be used if we were to reproduce the experiment documented in this paper, as it is possible that some cells were quiescent throughout a portion of our experiment without our knowledge. One means of getting a synchronized population of cells without quiescence is centrifugal elutriation. Cells are spun in an elutriation chamber, which can sort the cells based on size, with smaller cells forced into the proximal end and larger cells remaining at the distal end.[24] Assuming the largest cells are in G2 or M phase, they could be seeded on a gel for traction force microscopy and after they divide, their daughter cells could be tracked through a full cell cycle.
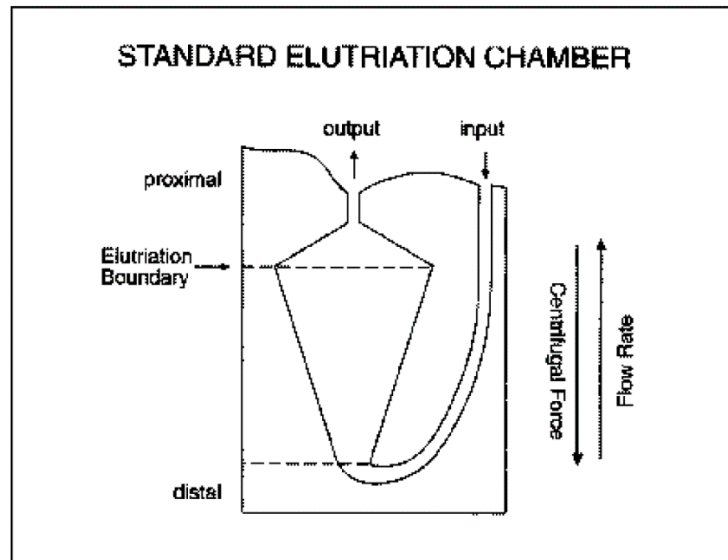
Figure 30: Schematic of an elutriation chamber. When cells are put into the chamber and it is activated, the cells will be sorted by size, with larger cells (G2 and M phase) aggregating at the distal end and smaller cells (G1 phase) at the proximal end.

Another advisement for future experimentation is to use conditioned medium in order to improve cell survival at low seeding densities. This would make the cells much easier to select and track, while also leaving ample room on the gel surface for the second generation of cells to adhere to and migrate across without too many coming into contact with one another.

References

1. Fox, S. I. (2009) *Human Physiology*. New York City, New York: McGraw-Hill.
2. Humphries, J. D., Byron, A., Humpries, M. J., Integrin ligands at a glance. *Cell Science at a Glance* **110** (19), 3901-3903 (2006).
3. Plow, E. F., Haas, T. A., Zhang, L., Loftus, J., Smith, J. W., Ligand Binding to Integrins. *The Journal of Biological Chemistry* **275** (29), 21785-21788 (2000).
4. Maniotis, A. J., Chen, C. S., & Ingber, D. E., Demonstration of mechanical connections between integrins, cytoskeletal filaments, and nucleoplasm that stabilize nuclear structure. *Proc. Natl. Acad. Sci. USA* **94**, 849-854 (1997)
5. Janmey, P. A., Winer, J. P., Murray, M. E., Wen, Q., The Hard Life of Soft Cells. *Cell Motility and the Cytoskeleton* **66**, 597-605 (2009).
6. Wang, J. H. & Lin, J., Cell traction force and measurement methods. *Biomechan Model Mechanobiol.* **6**, 361-371 (2007).
7. Discher, D. E., Janmey, P., Wang, Y., Tissue Cells Feel and Respond to the Stiffness of Their Substrate. *Science* **310** (5751), 1139-1143 (2005).
8. Georges, P. C., Janmey, P. A., Cell type-specific response to growth on soft materials. *Journal of Applied Physiology* **98** (4) 1547-1553 (2005).
9. Xiong, Y., Rangamani, P., Fardin, M., Lipshtat, A., Dubin-Thaler, B., Rossier, O., Sheetz, M.P., Iyengar, R., Mechanisms Controlling Cell Size and Shape during Isotropic Cell Spreading. *Biophys. J.* **98** (10) 2136-2146 (2010).
10. Califano, J. P., Reinhart-King, C. A., Substrate Stiffness and Cell Area Predict Cellular Traction Stresses in Single Cells and Cells in Contact. *Cellular and Molecular Bioengineering* **3** (1) 68-75 (2010).
11. Martin, B. M. (1994) *Tissue Culture Techniques.* Ann Arbor, Michigan: Braun-Brumfield Inc.

12. Metz, C. N., Fibrocytes: a unique cell population implicated in wound healing. *Cellular and Molecular Life Sciences* **60** (7): 1342-1350 (2003).

13. Palumbo, R., Sampaolesi, M., De Marchis, F., Tonlorenzi, R., Colombetti, S., Mondino, A., Cossu, G., Bianchi, M. E., Extracellular HMGB1, a signal of tissue damage, induces mesoangioblast migration and proliferation. *Journal of Cell Biology,* **179** (1): 33 (2007)
14. Kuo, M. I., Chapter X.11. Abscesses. *Department of Pediatrics, University of Hawaii John A. Burns School of Medicine*. University of Hawaii, March 2003. 16 January 2015 http://www.hawaii.edu/medicine/pediatrics/pedtext/s10c11.html
15. Muller, M., Cell Division, Mitosis, and Meiosis. *Department of Biological Sciences, University of Illinois at Chicago.* University of Illinois at Chicago, 2004. 16 January 2015 http://www.uic.edu/classes/bios/bios100/lecturesf04am/lect16.htm
16. Harris, A. K., Wild, P., Stopak, D., Silicone Rubber Substrata: A New Wrinkle in the Study of Cell Locomotion. *Science* **208** (11): 177-179 (1980).

17. Li, B., Xie, L., Starr, Z., Yang, Z., Lin, J., Wang, J., Development of Micropost Force Sensor Array with Culture Experiments for Determination of Cell Traction Forces. *Cell Motility and the Cytoskeleton* **64**, 509-518 (2007).

18. Franck, C., Maskarinec, S. A., Tirrell, D. A., Ravichandran, G., Three-Dimensional Traction Force Microscopy: A New Tool For Quantifying Cell-Matrix Interactions. *PLOS* **6** (3) e17833 (2011).

19. Schorl, C., Sedivy, J. M., Analysis of cell cycle phases and progression in cultured mammalian cells. *Methods in Cell Cycle Research* **41** (2) 143-150 (2007).

20. Konishi, T., Takeyasu, A., Natsume, T., Furusawa, Y., Hieda, K., Visualization of Heavy Ion Tracks by Labeling 3'-OH Termini of Induced DNA Strand Breaks. *Journal of Radiation Research* **52** (4): 433–440 (2011).

21. Damljanovic, V., Lagerholm, B.C., Jacobson, K., Bulk and micropatterned conjugation of extracellular matrix proteins to characterized polyacrylamide substrates for cell mechanotransduction assays. *Biotechniques* **39** (6): 847-851 (2005).

22. Ridley, A. J., Schwartz, M. A., Burridge, K., Firtel, R. A., Ginsberg, M. H., Borisy, G., Parsons, J. T., Horwitz, A. R., Cell Migration: Integrating Signals from Front to Back. *Science* **5** (302): 1704-1709 (2003).

23. Ridley, A. J., Hall, A., The small GTP-binding protein rho regulates the assembly of focal adhesions and actin stress fibers in response to growth factors. *Cell* **70** (3): 389-399 (1992)

24. Davis, P. K., Ho, A., Dowdy, S. F., Biological Methods for Cell-Cycle Synchronization of Mammalian Cells. *Biotechniques* **30** (6): 1322-1331 (2001)

25. Beningo, K. A., Dembo, M., Kaverina, I., Small, J. V., Wang, Y., Nascent Focal Adhesions Are Responsible for the Generation of Strong Propulsive Forces in Migrating Fibroblasts. *The Journal of Cell Biology* **153** (4): 881-887 (2001)

26. Fujita, J., Cold Shock Response in Mammalian Cells. *J. Mol. Microbiol. Biotechnol.* **1** (2): 243-255 (1999)

27. Sonna, L. A., Fujita, J., Gaffin, S. L., Lilly, C. M., Effects of heat and cold stress on mammalian gene expression. *Journal of Applied Physiology* **92** (4): 1725-1742 (2002)

28. Shojaeizadeh, M., An improved approach for cell traction force microscopy using a continuous hydrogel. *WPI Electronic Theses & Dissertations* (2013) https://www.wpi.edu/Pubs/ETD/Available/etd-060613-153345/

29. Lemmon, C. A., Chen, C. S., Romer, L. H., Cell Traction Forces Direct Fibronectin Matrix Assembly. *Biophysical Journal* **96** (2): 729-738 (2009)

30. Munevar, S., Wang, Y., Dembo, M., Traction Force Microscopy of Migrating Normal and H-ras Transformed 3T3 Fibroblasts. *Biophysical Journal* **80** (4): 1744-1757 (2001)

31. Mori, N., and K.A. Chang, Introduction to MPIV, user reference manual, p. 14. [Available at: http://www.oceanwave.jp/softwares/mpiv.] (2003)

32. Thomas, G., Burnham, N.A., Camesano, T.A., Wen, Q. Measuring the Mechanical Properties of Living Cells Using Atomic Force Microscopy. J. Vis. Exp. (76), e50497, doi:10.3791/50497 (2013).